光学学报

基于超表面的热辐射调控与红外应用(特邀)

尚效合[1]，仲帆[2**]，尚劲光[1]，张也[1]，肖彦玲[1]，祝世宁[1]，刘辉[1*]

[1]南京大学物理学院，固体微结构物理国家重点实验室，人工微结构科学与技术协同创新中心，江苏 南京 210093；

[2]东南大学物理学院，量子材料与信息器件教育部重点实验室，江苏 南京 211189

摘要　近年来，具有亚波长尺寸与超薄厚度的二维超表面结构以其灵活可控的光学响应，成功打破传统热辐射调控研究的瓶颈。目前，基于各种设计的超表面结构已实现了在波长、偏振、方向、时间和相干性等多个自由度上的热辐射调控，并促进了红外器件的小型化与集成化的发展。基于上述研究，回顾了近年来通过超表面调控热辐射的研究进展，并介绍了相应的红外应用发展，如红外传感、辐射制冷和热光伏器件等。

关键词　超表面；超表面阵列；热辐射调控；红外应用

中图分类号　TN214　　**文献标志码**　A　　**DOI**：10.3788/AOS241122

1　引　　言

热辐射是指温度高于绝对零度的物体由于带电粒子的无规则热运动而自发辐射电磁波能量的物理过程。热辐射现象在日常生活中随处可见。在19世纪，普朗克定律和斯特藩-玻尔兹曼定律相继被提出，从理论上描述了黑体辐射的物理过程。物体的热辐射能量与其辐射率ε和温度T有关，而黑体的辐射率固定为1。热辐射通常是宽带和非偏振的非相干光，传统材料难以精确地对热辐射进行多自由度的灵活调控，但是对热辐射的多自由度灵活调控对于各种红外应用至关重要。近20年来，随着纳米光子学和纳米制造技术的快速发展，对波长或亚波长尺度纳米结构的探索为热辐射多自由度灵活调控带来了突破。

目前多种人工微结构，如超表面[1-2]、超材料[3-4]、光子晶体[5-7]和多层结构[8]已被广泛地用于热辐射调控研究。与后三者相比，二维超表面具有超薄的厚度，并且可以提供空间上可调的辐射率，更有利于红外器件的集成化与小型化。近年来，超表面技术在包括红外热辐射场的光场多自由度(包括振幅[9-11]、相位[12-16]和偏振[17-19]等)调控方面展现了出色的能力，并实现了许多有趣的光学功能和应用，如超透镜[20-21]、生物化学传感[22-23]和光学吸收器[24-28]等。人工设计的超表面为热辐射多自由度调控提供了理想的研究平台，根据基尔霍夫定律，在热平衡条件下，互易热辐射器的辐射率等于其吸收率。因此，设计超表面的光吸收响应是调控其热辐射的关键。在过去的十多年里，研究人员对超表面吸收器[29-32]进行了广泛的研究。其中，多种超表面结构(如光栅[33-34]、微腔[35-36]、周期性排列的金属[37-38]和电介质[39-40]等结构)设计已被提出，用来调控光吸收和热辐射。通过对超表面元胞的合理设计，可在辐射波长、偏振、方向，以及空间和时间相干性等方面多自由度灵活调控热辐射。为了满足红外应用发展的需要，研究者们还提出了多种热辐射调控器件，如结合相变材料的动态可调热辐射器、违反基尔霍夫定律的非互易热辐射器、像素化热辐射阵列等。

本综述介绍了从单个超表面到像素化超表面阵列设计中的热辐射调控研究的最新进展。第2～4节介绍了在辐射光谱、偏振、辐射角度和相干性等多个自由度上调控热辐射的研究。第5节讨论动态可调的热辐射研究。第6节和第7节继续讨论违反基尔霍夫定律的非互易热辐射和近场热辐射的相关研究。第8节介绍基于热辐射调控的多种红外应用。此外，还分析红外器件应用领域中存在的问题与挑战。第9节介绍像素化热辐射阵列研究与其应用。最后，在第10节中对超表面调控热辐射的研究进行总结与展望。

2　波长选择性热辐射

首先介绍热辐射光谱调控的研究进展。传统的黑体辐射，例如白炽灯的辐射，通常具有覆盖整个红外波段的宽带辐射光谱，大部分辐射能量流入非需求的波段内，导致其在红外应用中的辐射效率较低。因此，在所需波段内实现波长选择性热辐射，同时尽可能地抑制其余波段的辐射，对于热光伏(TPV)和热管理器件

收稿日期：2024-06-02；**修回日期**：2024-07-20；**录用日期**：2024-07-30；**网络首发日期**：2024-08-10

基金项目：国家自然科学基金(12334015，92163216，92150302，62288101)、国家自然科学基金青年科学基金(12004072)

通信作者：*liuhui@nju.edu.cn；**zhongfan@seu.edu.cn

等红外应用至关重要。

当前，已有多种超表面[41-42]结构被提出，用于实现窄带选择性热辐射。其中，金属-电介质-金属（MIM）超表面[43-46]是常用的完美吸收器设计。该超表面由金属微结构、金属镜和它们之间的电介质层组成，金属层之间的磁共振可以实现完美吸收与辐射效果。因此，MIM超表面非常适合用于实现波长选择性的热辐射器件。Liu等[47]设计了一种具有窄带红外热辐射特性的MIM超表面，如图1(a)所示。此设计由顶部的十字形金（Au）谐振器、底部的金反射镜和它们之间的硅层组成。通过将不同尺寸的谐振器集成到一个元胞中，可进一步实现多共振热辐射。考虑到红外传感器件需要更窄的辐射峰，de Zoysa等[48]通过将多量子阱中的子带间跃迁模式与光子晶体共振耦合，在实验上实现了具有极窄带宽的热辐射峰，输入的能量可以被有效转化成窄带热辐射，进而实现高效的能量回收效果。

宽带辐射是辐射制冷、热伪装和热成像等红外应用所需的另一种辐射光谱调控需求。通过锥形、梯形超表面[49-52]或在超表面中组合多个共振微结构[53-59]，可实现宽带热辐射。Argyropoulos等[49]展示了一个基于锥形超表面的宽带热辐射器，如图1(b)所示。此宽带辐射特性来源于布儒斯特漏斗效应和绝热等离激元聚焦效应。在远离布儒斯特角时，超表面的辐射率会随之降低。Hossain等[50]提出了一种各向异性的圆锥形超材料结构，可以在大气透明窗口内产生非偏振的宽带红外辐射，如图1(c)所示，利用其独特的辐射特性，辐射器在环境温度下具有116.6 W/m^{2}的制冷功率。即使考虑现实环境中的非辐射热交换，超材料结构也能够在夜间冷却到环境温度以下（12.2 ℃）。

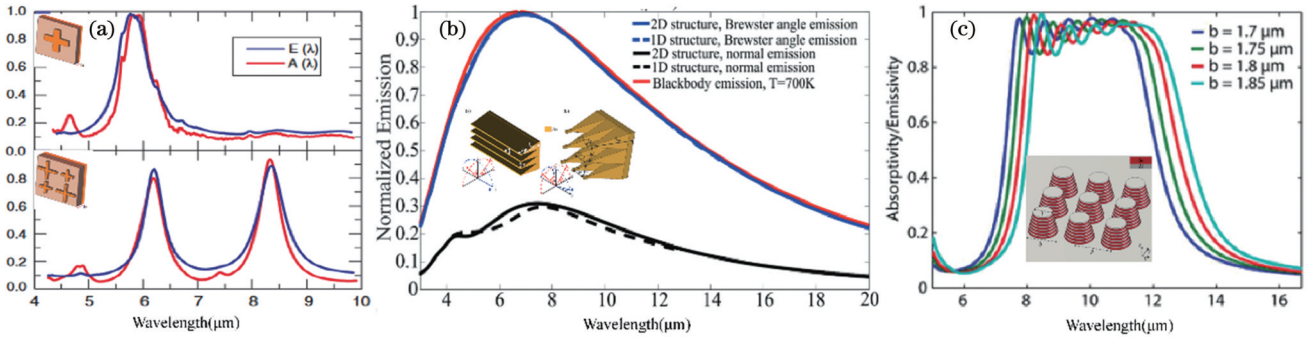

图1　波长选择性热辐射。(a)由一个或两个谐振腔组成的Au/Si/Au超表面的辐射光谱[47]；(b) T=700 K时一维和二维结构的归一化辐射光谱比较[49]；(c)测量的不同尺寸锥形超材料的辐射率（吸收率）[50]

Fig. 1　Wavelength-selective thermal emission. (a) Emission spectra of Au/Si/Au metasurfaces consisting of one or two resonators in a unit cell[47]; (b) comparison of the normalized emission spectra of 1D and 2D structures at T=700 K[49]; (c) measured emissivity (absorptivity) of the tapered metamaterial structures of different sizes[50]

上述超表面设计为热辐射光谱调控提供了详细的设计思路。波长选择性热辐射器可以用作高效、低成本的红外辐射源，为各种红外应用提供新的研究平台。

3　热辐射的偏振调控

非对称结构超表面的吸收光谱通常具有偏振依赖性。与非偏振的黑体辐射不同，这种超表面的辐射光谱会展现明显的偏振选择特性。

天线超表面结构可以产生平行或垂直于天线的线偏振热辐射。Schuller等[60]设计了一种碳化硅天线作为窄带红外辐射源。所设计的热辐射天线支持多个金属型和电介质型共振，这些共振模式可分为横电（TE）和横磁（TM）线偏振模式，其共振波长和偏振特性可以通过结构尺寸进行调控。Liu等[61]提出的天线结构的辐射功率峰值可以通过控制波导损耗或弯曲天线结构实现，使其趋近于黑体辐射极限，如图2(a)所示。除了天线辐射器外，许多超表面结构在线偏振入射下激发的高吸收也可以用来产生线偏振热辐射，如光栅[62-63]和矩形贴片超表面[44]。Mason等[63]提出了一种由金光栅、电介质层和金反射镜组成的波长选择性热辐射器，该结构在TM偏振光入射下的光栅和金属反射镜的反平行表面电流产生磁矩耦合，在特定波长下表现出强共振吸收。根据基尔霍夫定律，从被加热样品的表面就可以探测到线偏振的热辐射信号。

除了上述提到的线偏振热辐射，多种超表面结构还可以用来产生圆偏振热辐射。由于天然材料的手性响应非常弱，通过设计手性或非手性两种类型的超表面[64-67]可以产生圆偏振热辐射，如具有固有非互易特性的Weyl半金属、双曲超材料、手性纳米结构的手性效应、Rashba效应等。Dahan等[67]在实验中利用非手性天线超表面阵列产生了圆偏振热辐射。天线阵列在空间中的取向变化导致自旋分裂色散，相应的自旋相关辐射光谱如图2(b)所示。手性超表面[68-69]是另一种通过引入对称性破缺来有效增强手性响应的常见方法。手性超表面吸收器非常适用于产生圆偏振热辐

射。Nguyen等[70]展示了一种由连通的z字形谐振器组成的超薄白炽手性超表面，该超表面可实现宽带圆偏振热辐射，如图2(c)所示。在5～7 μm范围内，手性超表面的辐射信号偏振度大于0.5，并且通过电加热可以实现10 MHz的辐射调制速率。这种设计可以同时实现对中红外辐射源的光谱、偏振和调制速率的调控。到目前为止，大多数产生的圆偏振热辐射集中于超表面的法线方向上或呈现出定向辐射模式，非定向的圆偏振热辐射仍未实现。为了解决这一问题，Wang等[71]展示了一种对称性破缺的手性超表面，通过同时打破镜面对称性和空间反演对称性，实现了非对称的圆偏振热辐射，如图2(d)所示。所提出的手性超表面可以作为具有广角特性的中红外窄带圆偏振辐射源，未来有望集成于紧凑型芯片设计中。

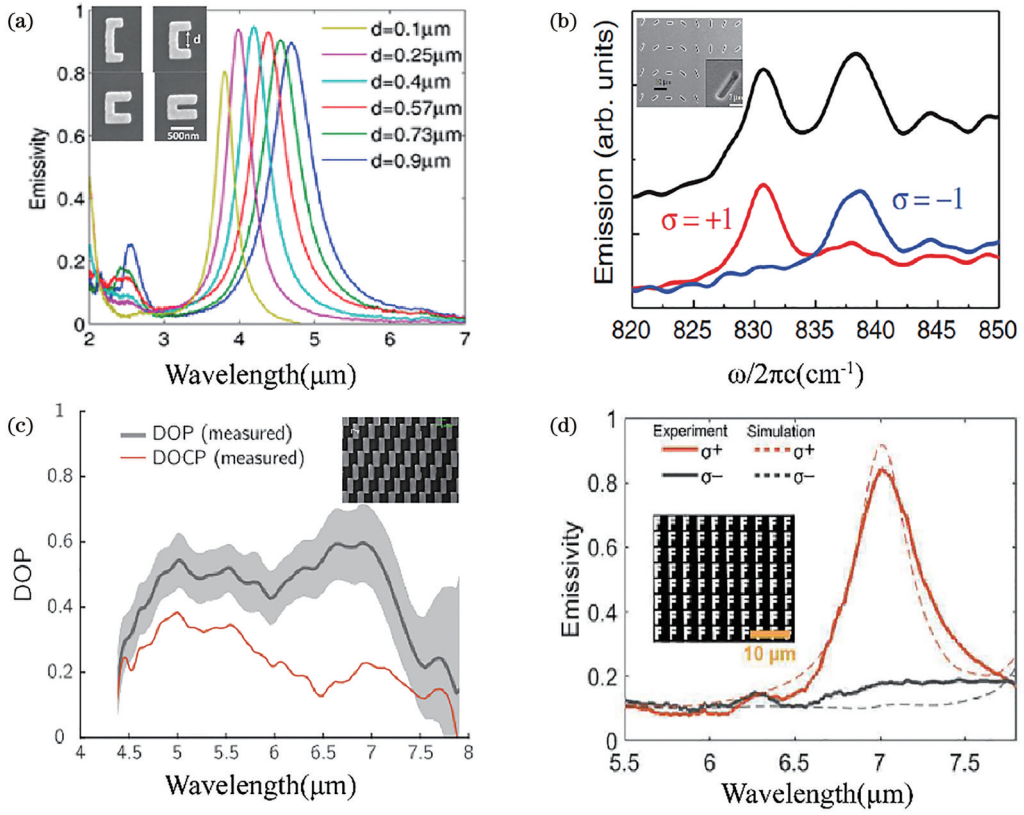

图2　热辐射的偏振调控。(a)实验测量得到的不同间距d的C形谐振器阵列的偏振辐射谱[61]；(b)无偏振片(黑线)、有右旋(蓝线)和左旋(红线)圆偏振片的热天线阵列的辐射谱[67]；(c)通过测量圆偏振热辐射得到的白炽灯手性超表面的偏振度(DOP)和圆偏振度(DOCP)[70]；(d)设计的F形手性超表面在左旋和右旋圆偏振下的辐射谱[71]

Fig. 2　Polarization control of thermal emission. (a) Experimentally measured polarized emission spectra of the C-shape resonator arrays with different d[61]; (b) measured emission spectra of thermal antenna array without a polarizer (black line), with right-handed circular polarizer (RCP, blue line), and with left-handed circular polarizer (LCP, red line)[67]; (c) obtained DOP and DOCP of incandescent chiral metasurface from measured circularly polarized thermal emission[70]; (d) measured emission spectra of designed F-shape chiral metasurface under left- and right- handed circular polarizations[71]

这些具有超薄厚度的手性和非手性超表面结构为设计线偏振或圆偏振片上热辐射器件提供了指导。热辐射偏振的调控能力对于红外辐射源、红外成像和红外传感等应用的发展具有重要意义。

4　热辐射的方向调控

4.1　辐射角度与空间相干性调控

一般来说，热源的热辐射在自由空间中是全方向的辐射。对热辐射角度调控的研究也是当前的一个重要问题。对热辐射角度的调控实际上是对热辐射空间相干性的调控，能否实现定向辐射的关键在于各个辐射点源的辐射相位是否具有固定关系。对此，研究人员提出基于极性材料中的声子极化激元[72-74]和金属光栅中的表面等离激元[75-76]的机制来调控热辐射的角度响应。

常用的白炽热光源发出的辐射具有宽带和非定向的特点，由于大部分辐射流入不需要的波段或方向内，光源的工作效率较低。通过将表面波与传播模式耦合，可以增强热辐射的相干性。2002年，Greffet等[77]开创性地提出了基于碳化硅(SiC)光栅的相干热源。热激发近场表面声子极化激元可以通过波矢动量匹配选择性地激发辐射来实现并产生角度依赖的辐射率，

从而实现了窄立体角红外辐射光源。此后，基于光栅[78-80]、金属沟槽[81]、周期微结构阵列[82]等各种超表面结构，研究人员进行了从定向热辐射到热聚焦等相干热辐射方面的理论研究。热激发表面等离激元是提高热辐射相干性而不受波长范围限制的一种常用方法。Han等[83]从理论上证明了周期性分布的圆形金属沟槽能够在狭窄的角度范围内向法向辐射窄带光束，如图3(a)所示。随后，Park等[84]通过在钨和钼薄膜上制作一系列同心圆形凹槽，从实验上验证了该理论设计在实现高定向热辐射方面的可行性。当加热至900 ℃时，钨制牛眼结构在垂直于结构平面的方向上可辐射出窄带且高度定向的红外光。Costantini等[85]提出了一种金/氮化硅/金的MIM超表面来实现窄带定向热辐射，如图3(b)所示。为了提高该MIM设计在高温下的稳定性，实验样品中的金被替换为钨。结果表明，在有限的立体角范围(0.84 sr)内，测量的辐射光谱是具有200 nm半峰全宽的高品质因子(Q)辐射。该MIM超表面在4.25 μm处具有较高的辐射率，在法向上满足临界耦合条件。当入射角增大时，该MIM超表面会出现更高阶的衍射级，为模式辐射提供新的衍射通道，不再满足临界耦合条件，导致辐射率下降。这就是窄带定向热辐射产生的原因。

部分相干性可以产生定向热辐射，但对热辐射振幅、偏振、局部相位和相干性的完全调控仍然困难。为解决该问题，Overvig等[86]从理论上提出了一种热超表面技术，设计了具有对称性控制非局域准连续域中的束缚态(QBIC)模式和局域模式的超薄双层电介质超表面，利用设计的自旋和角轨道动量实现热辐射聚焦和波前控制，如图3(c)所示。该技术利用了局域和非局域模式，使用局域模式可对波前进行整形，而非局域模式增加了热辐射的相干性。然而，对于实现热辐射聚焦[87]和热全息[88]的热辐射波前控制，目前还缺乏明确的实验。

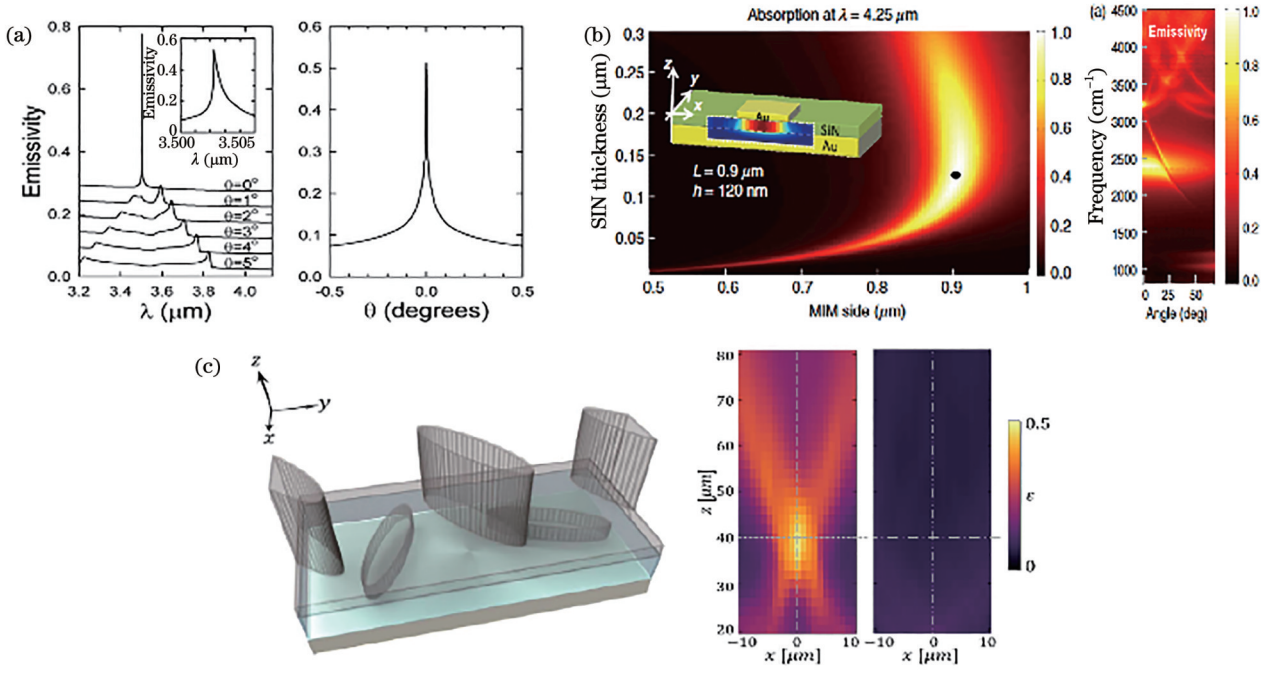

图3　热辐射的角度特性调控。(a)根据表面法向计算出钨牛眼结构在不同角度处的辐射谱，以及最大波长处辐射率的角度依赖性[83]；(b)二维MIM方形光栅随氮化硅(SiN)厚度变化的计算吸收谱和实验测量的超表面随角度变化的热辐射[85]；(c)热超表面的透视图及其在带边波长和非共振波长下辐射光的轮廓[86]

Fig. 3　Tuning of angular properties of metasurfaces. (a) Calculated emissivity spectra at various angles from the surface normal and angular dependence of emissivity at the peak maximum wavelength for a tungsten bull's eye structure[83]; (b) calculated absorption of a 2D MIM square grating as a function of the SiN thickness, and measured angle-dependent thermal emission of the metasurface[85]; (c) perspective view of thermal metasurface and its profiles of emitted light for the band-edge wavelength and nonresonant wavelength[86]

4.2　热辐射角度响应机制与角分辨热辐射光谱测量技术

通过引入模式耦合机制[89-92]，可以进一步丰富调控热辐射角度响应的手段。例如，在极性介质中，MIM共振和声子模式之间的耦合可以用来调控角辐射模式。Zhang等[93]利用铝/二氧化硅/铝超表面内部的耦合机制调控热辐射的带宽、偏振和角度特性，如图4(a)所示。在TE模式(平行于光栅的电场)入射下，该超表面只存在声子共振峰，呈现出角度依赖的辐射模式。与此相反，在TM模式(垂直于光栅的

电场)入射下,超表面会激发并耦合SiO_2层内的声子共振。利用等离激元-声子耦合增强的声子的热辐射,呈现出了极化的广角辐射模式。具有强远场辐射的亮模式和具有弱远场辐射的暗模式之间的耦合可以导致高Q的法诺共振。这种耦合方法可用于热辐射器中,以实现远场辐射模式可调节的窄带热辐射。Zhang等[94]基于铝/氮化硅/铝超表面提出了一种法诺共振型热辐射器。这种法诺共振是由奇偶对称暗磁共振模式与表面晶格(SLR)模式耦合引起的。通过调整结构尺寸和周期性以及暗模式和亮模式的重叠可以形成法诺共振,从而在法线方向上产生非常窄的热辐射峰。为了通过实验证明其辐射特性,他们基于傅里叶红外光谱仪(FTIR)提出了一种角度分辨热辐射光谱(ARTES)技术,将样品固定在旋转加热台上,利用加热窗口采集旋转样品的辐射信号,在窗口前放置红外偏振片以选择所需的热辐射偏振,最后用FTIR进行信号分析。角分辨热辐射结果如图4(b)所示,可以看出,随着光栅宽度的增加,超表面会产生法诺共振,呈现窄带定向热辐射的特性(虚线圆圈)。

上述ARTES技术是热辐射光谱角度响应表征的强力工具。Zhong等[95]利用ARTES技术直接表征了设计的超晶格色散,证明了非厄米系统的固有本征模式特性,如图4(c)所示。在高度h_b=0.8755 μm下的超晶格结构和测量的热辐射结果表明了异常点的存在。此外,该ARTES技术还可用于探测中红外表面波的辐射。Zhong等[96]通过测量的热辐射色散证明了超晶格上表面波的存在,如图4(d)所示。自行搭建的角度分辨热辐射光谱测量系统具有良好的角分辨能力和从近红外到远红外的宽频率工作范围,并且这种探测方法不需要红外光源激发即可探测红外表面波,可以在合成维度空间研究新奇的物理现象,例如连续域中的束缚态(BICs)、体费米弧和异常线等。

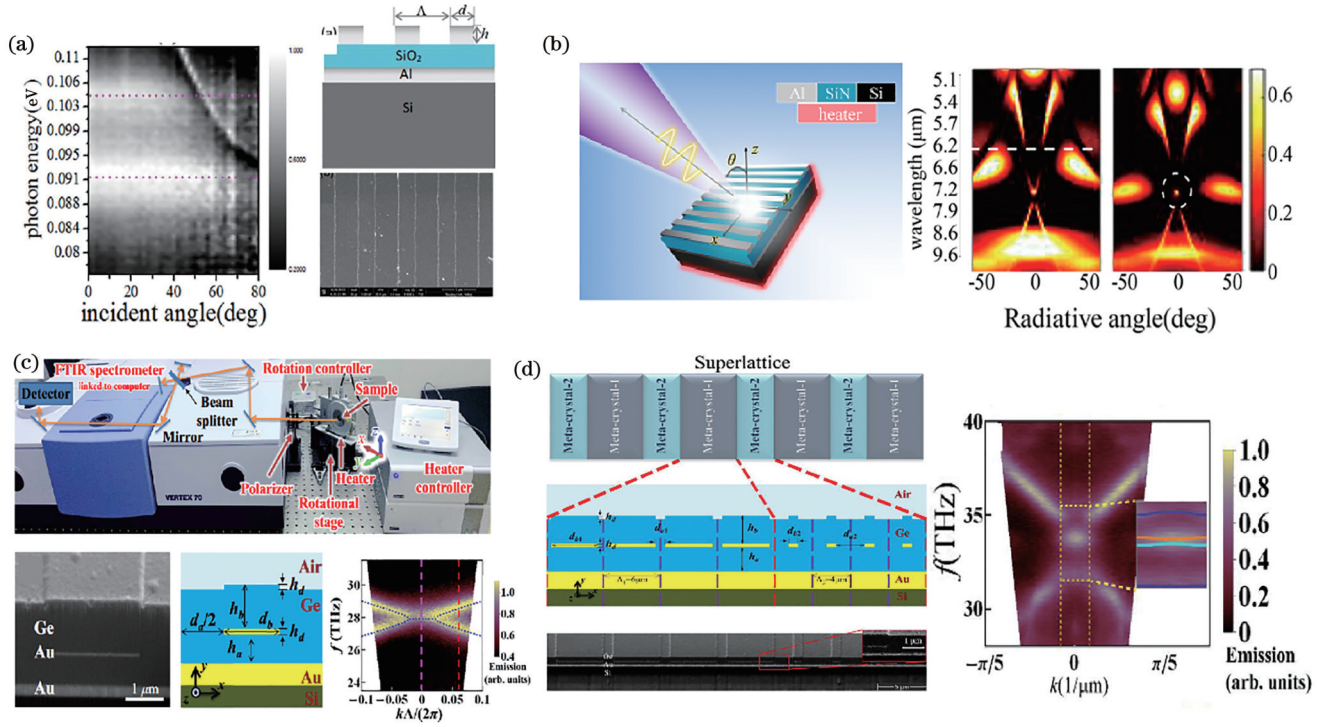

图4　热辐射角度响应机制与角分辨热辐射光谱测量技术。(a)设计的Al/SiO_2/Al超表面,以及测量得到的TE和TM偏振下随角度变化的热辐射[93];(b) Al/SiN/Al超表面示意图,以及测量的角度分辨热发射随光栅宽度d的增加(白线和圆分别表示暗磁共振模式和法诺共振点)[94];(c)上图为角分辨热辐射光谱测量装置示意图;下图从左至右依次为制备样品的扫描电子显微镜(SEM)图,设计的超晶格示意图,测量和计算的热辐射色散[95];(d)设计的超晶格示意图和SEM图,并测量和计算了热辐射色散,表明界面态的存在[96]

Fig. 4　Mechanism of thermal radiation angle response and angle-resolved thermal emission spectroscopy. (a) Designed Al/SiO_2/Al metasurface and measured angle-dependent thermal emission under TE and TM polarizations[93]; (b) sketch plot of Al/SiN/Al metasurface and measured angle-resolved thermal emission varying with increasing grating width d (white line and circle indicate the dark magnetic resonance mode and the Fano resonance point)[94]; (c) the top image is ARTES measurement setup, and bottom images from left to right are SEM picture of the fabricated sample, the schematic of designed meta-crystal, and measured and calculated thermal emission dispersions[95]; (d) sketch and SEM picture of the designed superlattice, and measured and calculated thermal emission dispersions, indicating the existence of interface states[96]

5 热辐射的动态调控

到目前为止，讨论了热辐射对波长、偏振和角度等特性的调控，然而，大多数的超表面设计是静态的，其辐射特性是由结构参数决定的。通过在结构中加入光学特性可调的材料或者引入外部动态调控机制可以实现热辐射的动态调控。近年来，高速调制下具有可切换热辐射特性的动态可调控热辐射器在空间可重构热成像和自适应热伪装等自适应热管理器件的发展中受到了广泛关注。利用石墨烯[97-104]、砷化铟(InAs)[105]、砷化镓(GaAs)[106]、氮化镓(GaN)[107]等活性材料和各种相变材料[如二氧化钒(VO_2)[108-112]、GST($Ge_2Sb_2Te_5$)[113-115]等材料[116-117]]，可以实现辐射特性的动态调控。相应地，许多动态调控机制被深入探究，包括电调控[118-120]、温度调控[121-122]、机械调控[123]、紫外线(UV)照射[124]、飞秒激光脉冲激发和加热[125-126]等。

石墨烯具有热质量小、导热系数大的特点，是一种极具发展前景的片上热敏材料和高速热敏材料。多层石墨烯可以作为白炽灯热源，提供连续的红外辐射光谱。石墨烯谐振器或结合石墨烯层的金属超表面能够在红外范围内产生等离激元共振，从而实现波长选择性热辐射。Brar等[98]通过实验展示了一种由石墨烯天线、SiNx膜和Au反射镜组成的可控窄带热辐射器。通过改变石墨烯的载流子密度，可以连续调控天线的辐射波长和强度。InAs、GaAs和GaN等活性材料也被用于实现动态热辐射调控。例如，Kang等[107]展示了在高达500 ℃的温度下基于GaN/AlGaN多量子阱结构以高调制速度(50 kHz)实现的电调制的窄带中红外热辐射器，其辐射强度可由量子阱结构中的电子密度调控，如图5(a)所示。

实现动态调控热辐射的另一类方案是使用相变材料，例如GST和VO_2，由于其超快的调制速度和可重复的温度循环而被广泛研究。相变VO_2材料在68 ℃左右会经历绝缘体到金属的相变，与GST的高温相变不同，近室温的相变温度使得VO_2适用于航空电子设备和类似的电子元件。Chandra等[109]通过实验展示了一种自适应红外伪装系统，由于相变会引起VO_2的介电常数发生变化，通过改变有效腔厚度就可以改变腔耦合等离激元超表面的红外辐射率。他们演示了在像素化超表面上编码红外信息的自适应伪装，从而促进热伪装的多光谱和空间红外信息编码的发展。与VO_2材料相比，GST材料可以以非晶态和晶态存在，并且可以通过快速和慢速退火来回切换，其慢速结晶过程需要500 K的温度条件，快速结晶过程需要750 K才能从非晶态相向晶态相转变。一旦相变完成，非晶态或晶态可以在室温下保持很长一段时间，这有利于节能的热器件设计，例如Qu等[113]提出了一种低功耗的中红外热辐射器，结合相变材料GST实现了零静态功率动态控制，通过控制GST结晶的温度，可以连续调节辐射率、带宽和峰值波长。

将活性材料与可重构调控机制相结合，可大大丰富热辐射器的调控自由度，实现光谱、空间和时间的热辐射调控。Liu等[123]将微机电系统(MEMS)与超材料相结合，基于可重构的设备实现了对热辐射能量的控制，如图5(b)所示。该系统能够在不改变温度的情况下通过施加偏压引起的静电力控制结构尺寸，从而调控表面辐射率。与其他改变其动力学温度或化学成分的方法不同，MEMS辐射特性是通过其几何参数变化调节结构中电共振和磁共振的耦合，从而实现能量控制。这一概念可用于构建具有可重构性的MEMS超材料像素表面，从而实现能够以高达110 kHz的调制速率显示的热红外图案。通过紫外光照射方法，可以实现超表面辐射率的时间和空间同步调控。Coppens等[124]通过将MIM超表面与光敏材料氧化锌(ZnO)结合，可以实现光谱和时空辐射率的控制，如图5(c)所示。ZnO层具有较长的光载流子寿命，允许通过低功率、连续波照明来调制辐射率。为了提高调制性能，Xu等[126]最近提出了一种非易失性光学可重构中红外编码辐射超表面，如图5(d)所示。相变材料GST的引入实现了红外发射的可重构性和动态控制。GST中的非易失性相变使该编码超表面成为节能的零静态功率器件。此外，激光调制GST相变和激光诱导微尺度凸起能够独立或同时控制中红外热辐射和可见光散射特性。这种方法是热辐射调控的新途径，在红外数据存储、加密和伪装等方面具有广泛的应用。

结合各种活性材料、相变材料和外部调控机制，如激光调制和电调制，可以实现多自由度的动态热辐射调控，进一步丰富调控自由度和提高调制速度是研发下一代自适应热管理器件的关键。

6 非互易热辐射

基尔霍夫定律提出：在给定波长(λ)、偏振(p)和方向(θ)下的吸收率α和辐射率e是相等的，即$\alpha(\lambda,p,\theta)=e(\lambda,p,\theta)$。这个定律来源于麦克斯韦方程组的洛伦兹互易性。该定律仅在非磁性材料、时不变系统和线性材料中有效。因此，可以通过改变这三个条件中的任何一个来实现非互易辐射和吸收，即使用磁响应材料、时变系统或光学非线性材料。非互易热辐射的调控对太阳能电池、辐射制冷和热光伏等光子能量转换技术非常重要。以太阳能收集系统为例，为了保证太阳能的吸收效率，需要收集系统对太阳光有较高的吸收率，根据基尔霍夫定律，互易的热辐射就会不可避免地返回太阳，这增加了系统的固有损耗。因此，非互易系统[127-130]对于太阳能收集系统达到其效率极限(即兰德斯贝格极限)具有重要意义。

在强磁场下，能提供不对称介电常数张量的磁光(MO)材料[131-132]可以用于实现非互易热辐射。2014

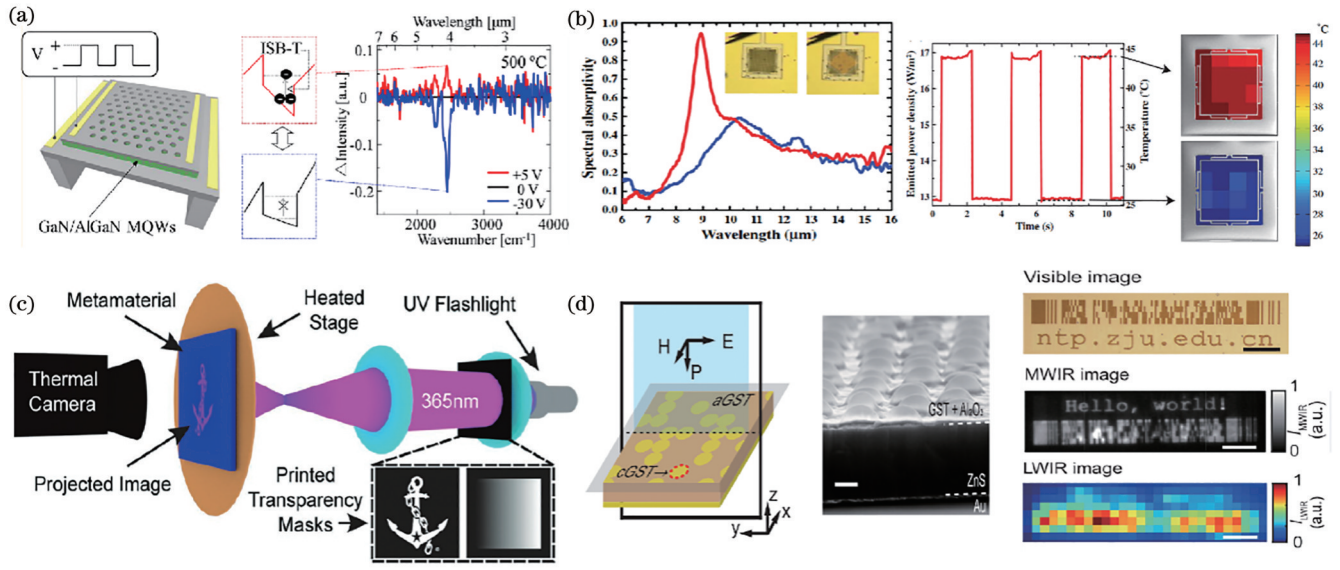

图 5　热辐射的动态调控。(a)基于 GaN/AlGaN MQW 的可控热辐射器示意图，以及 0 V 和非 0 V 电压下的热辐射强度差[107]；(b)在开启(红色曲线)和关闭(蓝色曲线)状态下测量到的超材料辐射器的光谱吸收率以及单像素超材料发射器成像测量结果[123]；(c)利用紫外线投影图像展示空间辐射率的调控[124]；(d)左图为通过控制 cGST 点密度来调制辐射率的示意图，扫描电镜(SEM)图像显示了由纳秒激光脉冲产生的亚微米大小的凸起，右图为不同波长范围的二元防伪标签[126]

Fig. 5　Dynamic control of thermal emission. (a) Schematic of electrically controllable GaN/AlGaN MQW photonic crystals based thermal emitters, and difference between the thermal emission intensity spectra at 0 V and nonzero applied voltages[107]; (b) measured spectral absorptivity of the metamaterial emitter in both on (red curve) and off (blue curve) states, and imaging measurement result of the single-pixel metamaterial emitter[123]; (c) demonstration of spatial emissivity control using UV projected images[124]; (d) left image shows the emissivity modulation by controlling the density of cGST points, SEM image shows the submicron-sized bumps fabricated by ns laser pulses, and right image shows binary anticounterfeiting label in different wavelength ranges[126]

年，Zhu 等[133]从理论上提出了一种磁光 InAs 光栅，实现了最大限度违反基尔霍夫定律的效果，如图 6(a)所示。在沿 z 轴 3 T 的强磁场和临界耦合条件下，系统在 15.96 μm 波长处的辐射率和吸收率对比度高达 10.2 dB。为了降低非互易系统对磁场的依赖性，Zhao 等[134]证明了无损光栅中的导模可以有效地增强磁光效应，从而将对磁场的要求降低到 0.3 T。使用磁光材料实现非互易热辐射仍需外部磁场的辅助，磁性外尔半金属[135-136]由于其固有的时间反演对称性破缺和独特的拓扑非平凡电子态性质，成为非互易系统的研究热点。Zhao 等[135]展示了一种由磁性外尔半金属光栅组成的非互易热辐射器，如图 6(b)所示。该非互易热辐射器在不需要外加磁场的情况下，其介电常数张量非对角线项存在非零贡献，实现了非互易热辐射。由于 $e(\lambda,\theta)=\alpha(\lambda,\theta)$，因此非互易热性质对于吸收率具有较强的角度依赖性，然而，上述提到的磁性材料的介电常数具有各向异性，磁导率具有各向同性，因此只能得到 TM 极化的热辐射信号。除了磁光材料和磁性外尔半金属外，利用不对称散射矩阵进行时空调制是违反基尔霍夫定律的另一种方式。研究人员已经提出了天线[137]和光栅[138-139]的时空调制，以实现兆赫和长波红外范围内的非互易效应。Ghanekar 等[138]提出了一种特定的光栅设计，该光栅结构在斜入射条件下表现出不对称的定向反射，如图 6(c)所示。对于与临界耦合相对应的调制深度，计算结果表明方向不对称的散射矩阵违反基尔霍夫定律，即对于给定的频率和入射角，吸收率不等于发射率。

以上提到的研究均为理论研究，未进行实验验证。天然磁光材料中的物质损耗会引起弱非互易效应，导致在之前的工作中需要大磁场或高品质因数谐振才能实现非互易热辐射。最近，Shayegan 等[140]通过实验观察，从测量的吸收和辐射光谱中发现了违反基尔霍夫定律的现象。通过将介质光栅的导模共振(GMR)与磁光材料 InAs 耦合，可以在磁场调控下打破介电常数张量的对称性。当外加磁场从 1.0 T 切换到 −1.0 T 时，测得的辐射率和吸收率变化满足 $\Delta e=-\Delta\alpha$(其中 Δe 为辐射率变化，$\Delta\alpha$ 为吸收率变化)的关系，显示出了相同角度下的非互易辐射特性。在 n-InAs 的介电常数趋于零(ENZ)的波长处，非互易效应最强，并可扩展到其他波长范围。这个工作为未来非互易热辐射器的实验工作开辟了道路。

此外，利用非线性材料也可以打破洛伦兹互易性。其中，克尔 $\chi^{(3)}$ 非线性可以用来调控热辐射。Khandekar 等[141]提出了一种非线性四波混频方案用于

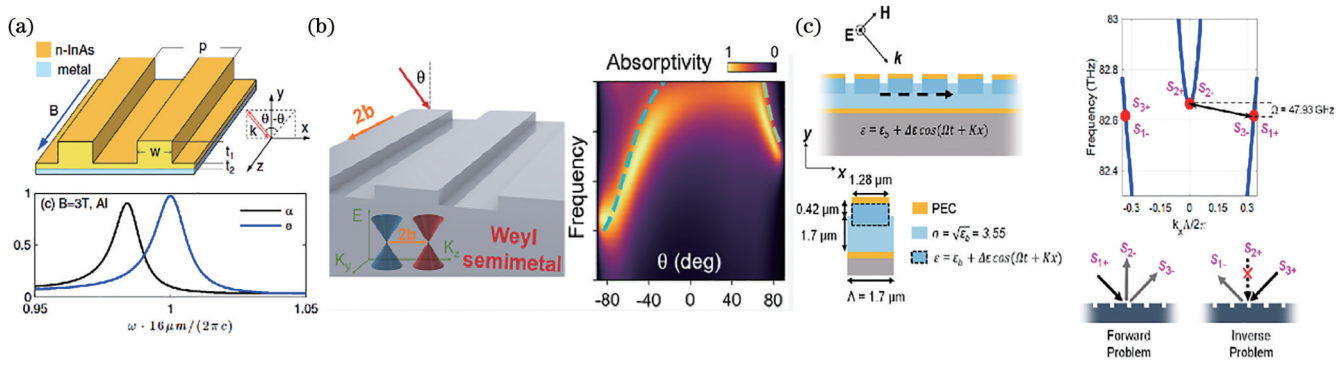

图 6　非互易的热辐射调控。(a)由 InAs 光栅和金属层组成的非互易热辐射器的示意图，在入射角度 θ=61.28°和磁感应强度 B=3 T 条件下非互易热辐射器的计算吸收光谱和辐射光谱[133]；(b)外尔半金属光栅示意图(该结构与角度相关的吸收率显示出明显的不对称性质)[135]；(c)左图展示了导模共振光栅随时间的调制的折射率变化状况，右图突出显示感兴趣的共振模式[138]

Fig. 6　Nonreciprocal thermal emission control. (a) Sketch of the nonreciprocal thermal emitter composed of InAs grating and metal layer and calculated absorptivity and emissivity spectra of the nonreciprocal thermal emitter at the condition of incident angle θ=61.28° and B=3 T[133]; (b) schematic of the Weyl semimetal grating (the angle dependent absorptivity, showing clear asymmetric properties)[135]; (c) left image shows the change of refractive index caused by the modulation of the guided mode resonance grating over time, and right image shows resonance modes of area-of-interest[138]

实现近场的热转换和能量转移，以证明在各种间隙尺寸(从数十到数百纳米)内系统可以在工作温度下以低强度进行高效热制冷，并进一步利用该方案来实现不同温度下物体之间近场热交换的幅度和方向可调性。几乎所有涉及线性响应材料的热辐射现象都可以利用半经典光理论解释，热光子的非线性在理论上是一个具有挑战性的研究问题，它与热辐射、可再生能源和能源转换技术的应用相关。Khandekar 等[142]提出共振增强的非线性相互作用能够通过上转换选择性增强热辐射，热辐射超越了与线性介质相关的黑体极限，使用非线性介质调控热辐射是一个新兴课题。

打破洛伦兹互易性是调控非互易热辐射的独特方式，为热光伏和新型热光伏电池等非互易能源器件提供了更多的可能性，同时非互易热辐射的调控在单向传感器、热伪装和热隐身等领域也有重要的应用。

7　近场热辐射

热辐射是热交换中的三个基本通道之一，它可以在没有介质的情况下传播。在受普朗克热辐射极限限制的远场热辐射中，科研人员已经做了大量的工作。然而，亚波长热辐射器似乎超过了极限，其中一些违反直觉的现象是由于辐射截面和几何截面之间的差异造成的，而另一些现象的发生则是由内部的温度梯度造成的[143-144]。

研究人员已经在许多系统中对近场热辐射进行了理论研究，包括图像化的一维[145-150]、二维[151-152]纳米结构和基于二维材料的设计，如双曲纳米结构[153-156]和石墨烯平面[157-159]。Liu 等[151]从理论上研究了图像化超表面的近场特性，与非图像化薄膜相比，图像化一维和二维超表面支持的双曲模式与真空中的倏逝波之间的耦合可以增强近场传热，如图 7(a)所示。然而，这种近场传热比由极性电介质制成的平行板中的传热要弱。为了解决这一问题，Fernández-Hurtado 等[152]从理论上论证了一种基于硅超表面的近场辐射传热方法，在室温下，硅超表面的辐射传热比无图案的平面极性电介质强得多，如图 7(b)所示。在硅层中引入的孔导致了宽带表面等离激元的产生，从而在宽带范围(从 13 nm 到 2 μm)内增强了近场辐射传热。近场热辐射可以超过黑体极限几个数量级，特别是当存在表面模式或双曲模式时，近场热辐射的进一步增强和操纵具有广泛的应用前景。六方氮化硼(hBN)作为一种天然双曲材料可增强近场热辐射。然而，由 hBN 支撑的双曲声子极化激元的可调性是有限的。为了解决这个问题，Shi 等[155]提出了多层石墨烯-hBN 异质结构的混合设计以进一步增强近场热辐射，如图 7(c)所示。石墨烯由于其高度可调的载流子迁移率和强约束的表面等离激元而被广泛应用于近场传热系统。例如，热传导的“ON”和“OFF”切换状态可以在堆叠的石墨烯片中实现[157]。Ilic 等[158]从理论上证明了一种基于石墨烯热激发表面等离激元的近场辐射热开关，石墨烯的高可调性能够对近场辐射传热进行大幅调制，如图 7(d)所示。

为了观测近场热辐射，实验中需要可读的近场热辐射信号[160-164]。一种解决方案是利用散射型扫描近场光学显微镜(s-SNOM)提取近场信号。Kajihara 等[160]在没有外界照明的情况下，用 s-SNOM 法检测 300 K 的样品，得到了约 60 nm 的高空间分辨率的近场信号。将样品发出的近场热辐射信号引导至傅里叶变换红外光谱仪(FTIR)中，即可得到近场热辐射光谱[161]。另一种基于高精度 MEMS 的方法为定量揭示纳米梁之间的近场辐射传热提供了机会。St-Gelais

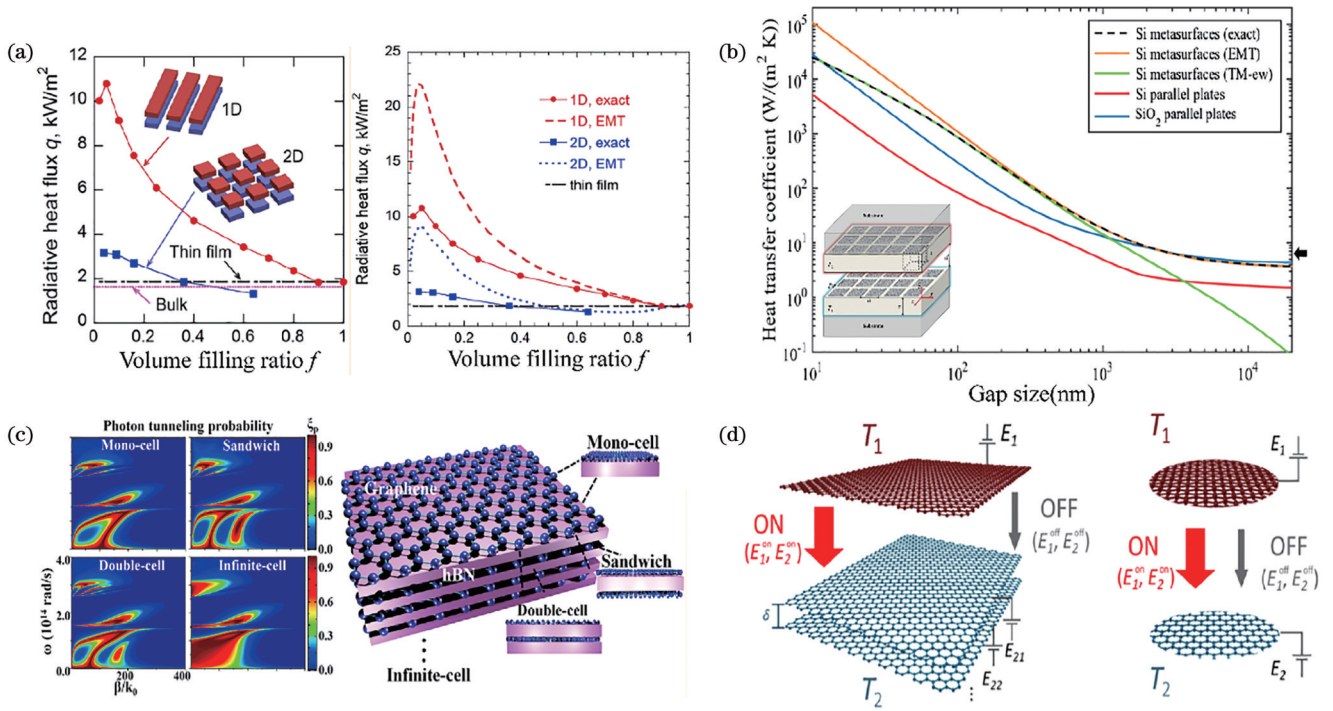

图 7　近场热辐射调控。(a)一维和二维超表面之间的近场热辐射示意图以及辐射热通量与体积填充比的函数变化关系[151]；(b)两个掺硅超表面的近场换热示意图，以及 Si 超表面、Si 和 SiO_2 平板的室温换热系数随间隙大小的变化规律[152]；(c)无限石墨烯-hBN 异质结构示意图。单细胞、夹层和双细胞结构及其相应的光子隧穿概率[155]。(d)堆叠的石墨烯片在“开”和“关”状态之间提供了更好的导热对比[158]

Fig. 7　Near-field thermal emission control. (a) Schematic of near-field thermal emission between 1D and 2D metasurfaces and radiative heat flux as a function of volume filling ratio[151]; (b) schematic of two doped-Si metasurfaces for near-field heat transfer and room-temperature heat transfer coefficients of Si metasurfaces, and Si and SiO_2 parallel plates as functions of gap size[152]; (c) schematic of infinite graphene-hBN heterostructure. Monocell, sandwich, double-cell structures, and corresponding photon tunneling probability[155]. (d) stacked graphene sheets offer improved heat conductance contrast between “ON” and “OFF” switching states[158]

等[162]发现系统在纳米梁间距为 42 nm 的条件下的近场传热增强比远场极限大两个数量级。当距离小于 200 nm 时，传热遵循典型的 $1/d^{\alpha'}$ 规律，其中 d 为间距，α' 为几何依赖系数。纳米梁上的高拉伸应力使得即使在较大的热梯度下也能稳定地控制纳米级分离。此外，Yang 等[163]设计了一种自制的装置，该装置能够直接测量两片宏观石墨烯之间等离激元的近场热辐射。该测量系统可以保持两个石墨烯片之间的最小间隙约为(430±25) nm，在近场探测中具有良好的性能。石墨烯薄片的测量结果显示，其热流密度是黑体极限的 4.5 倍，表现出明显的超普朗克辐射。

对近场热辐射黑体极限的探索，为高分辨率近场成像、热整流器、热晶体管、热光伏器件等热辐射器件的研制开发以及能量收集和热管理方面的应用开辟了新的途径。此外，近场热辐射对于集成纳米机电系统和热电子器件的热控制至关重要[164]。

8　基于热辐射器件的红外应用

对热辐射调控的深入研究为许多红外应用如辐射制冷、热光伏、热成像、生化传感和热伪装器件等提供了坚实的基础。本节介绍了几种重要的基于热辐射器件的红外应用。

8.1　辐射制冷

地球大气层对电磁波的响应有两个透明窗口(3～5 μm 和 8～14 μm)，通过利用这个窗口，人们可以将地表的热量辐射到寒冷的外层宇宙空间中(3 K)。辐射制冷[165-172]是一种利用大气窗口的新兴技术，它可以在不消耗外部能量的情况下被动降温，为缓解能源和全球变暖等问题提供了一种极具前景的方法。夜间辐射制冷已被广泛研究，但是制冷的需求高峰主要出现在白天。因此，探索白天辐射制冷的策略具有重要意义。为了实现白天的辐射制冷，需要热辐射器在地球大气透明窗口内具有较高的辐射率，同时对太阳光波段具有较高的宽带反射率。Rephaeli 等[165]首先从理论上提出了一种基于金属-电介质光子结构的日间辐射制冷设计，如图 8(a)所示。该设计将集成的波长选择性热辐射器与宽带反射器结合，在增强大气窗口内热辐射的同时抑制了对太阳光的吸收，在环境温度下净制冷功率(单位面积的功率)超过 100 W/m²。Raman 等[166]通过多层光子结构实验演示了白天的辐射制冷效果，

可以实现比环境温度低4.9 ℃的降温效果和40.1 W/m^{2}的制冷功率。为了满足大规模商业应用和低成本的要求，Zhai等[167]提出了一种随机玻璃聚合物掺杂超材料设计，将二氧化硅微球随机分布在透明聚合物中，实现高效的全天辐射制冷，如图8(b)所示。由于微球的声子增强Fröhlich共振，该大规模设计实现了8～20 μm范围内的高红外辐射率和对太阳辐射的高效反射(约96%)，连续72 h测量的平均制冷功率高于110 W/m^2。此前大多数报道的辐射制冷材料都具有覆盖整个中红外波长范围的宽带辐射，Li等[170]提出了一种分层设计的基于聚合物纳米纤维的薄膜，通过可扩展的静电纺丝工艺生产，能够实现选择性中红外辐射和有效的阳光反射，从而实现了全天辐射制冷。该设计在8～13 μm范围内实现了选择性辐射(78%)，在0.3～2.5 μm范围内实现了有效的太阳光反射(96.3%)。与无选择性辐射器相比，这种选择性辐射制冷设计在夜间的冷却温度提高了3 ℃，在白天可以实现比环境温度低5 ℃的降温效果。这种设计为解决全球变暖提供了新的方案。

为了应对全球变暖和能源消耗的危机，结合被动辐射制冷设计的个人热管理技术得到了广泛的研究。Zeng等[171]提出了一种随机分散的散射体分层超构纺织物，如图8(c)所示。通过可扩展的工业纺织品制造路线，超织物表现出商业服装所需的机械强度、防水性和透气性，同时保持了高效的辐射制冷。实际应用测试表明，这种大型超织物在大气窗口表现出高辐射率(94.5%)，对太阳光谱表现出高反射率(92.4%)，覆盖超织物的人体温度可以比覆盖商业棉织物的人体温度低约4.8 ℃。与辐射制冷相比，辐射制热是另一种节能技术，它可以通过调节红外辐射光谱来实现被动抑制物体的热辐射，同时主动利用大气的热辐射制热[173]。这种辐射制热技术有助于应对气候变化的挑战，促进全球碳中和的实现。

8.2 热光伏设备

热光伏装置[174-185]由热源、热辐射器和光伏电池组成，是一种将热量转化为电能的新技术。通过热源，热辐射器可以达到高温，产生热辐射，最后由光伏电池将能量转化为电能。热源可由燃料燃烧、核反应、电过程和太阳辐射提供。由于能量低于PV电池带隙的光子不能被吸收并用来发电，因此需要波长选择性热辐射器来提供能量高于PV电池带隙的辐射光子。可以看到，热辐射器可以提高热电转换效率，在TPV系统中发挥着重要的作用。

利用太阳辐射作为热源，将太阳能转化为电能的能量转换系统被称为太阳能热光伏(STPV)系统。系统中利用了一个宽带太阳能吸收器来吸收太阳光子并加热。Chang等[174]通过实验展示了一种STPV装置，该装置结合了难熔的钨超表面太阳能吸收器和热辐射器，在至少1200 ℃的温度下仍具有良好的热稳定性，如图8(d)所示，实现了可见光至近红外波段的近均匀吸收和长波域的抑制辐射，提高了能量转换效率。整体STPV的效率高达18%，与现有的商用单结PV电池的效率相当。为了进一步提高TPV器件的实用性，提高系统的高温稳定性和TPV效率成为了当下亟待解决的问题。

8.3 气体探测和生化传感

许多分子在中红外波段表现出强烈的特征共振吸收，因此中红外气体探测和传感在工业检测和环境传感等领域具有重要意义。常用的红外光源如量子级联激光器通常结构复杂且价格昂贵，这限制了其在低成本光学气体传感方面的应用。热辐射作为一种高效紧凑、低成本的红外辐射源，在非色散红外传感和生化传感分析中具有很高的应用价值。对于气体传感应用[186-190]，热辐射器可以在不需要额外滤光器件的情况下提供目标辐射峰，从而促进了传感装置的小型化。例如，Lochbaum等[46]展示了一种适用于中红外波长范围的高效、窄带片上热辐射器，通过将MEMS加热器技术与超材料辐射器结构相结合，利用窄带热辐射器作为波长选择性红外辐射源，实现了无滤波器、低成本和紧凑的气体传感。此外，通过在非谐振腔内集成基于超表面的辐射器和探测器，Lochbaum等[189]提出了一种更紧凑的中红外气体传感器。该中红外气体传感器可以实现$(22.4\pm0.5)\times10^{-6}\ \mathrm{Hz}^{-0.5}$的$CO_2$灵敏度，其设备性能可与现有的商用设备相媲美，每次测量时消耗的能量可减少80%，克服了传统非色散红外传感器的集成限制难题。

芯片上的生化传感[191-193]也可以通过宽带热辐射器进行探索。从热辐射器辐射的热光与所检测样品的相互作用或通过所检测样品传输，将分子化学键的振动信息传递到光谱仪中。然后通过测量光谱在有/无样品情况下的变化，提取被检测样品的特殊振动信息。超表面同时作为辐射源和传感器芯片，可以大大简化实验装置，有利于气体探测器件和生化传感器件的紧凑化和小型化，低成本的优势使其也更具应用前景。

8.4 热伪装

热伪装是一种自然行为，像变色龙这样的生物，为了躲避捕食者或猎物，通过热伪装融入周围环境。与自然伪装相似，热伪装[194-205]实现了从红外探测器中隐藏目标物体，在许多领域具有很大的实用价值，如军事和防伪设备等。控制表面辐射率是防止热辐射信号被热像仪等各种红外探测技术探测到的有效方法。传统的热伪装只能在特定的背景温度下工作，这使得动态可控热伪装在实际应用中更具吸引力。Salihoglu等[194]设计了一种基于多层石墨烯的实时主动热表面，通过可逆插入非挥发性离子液体，热表面可以在不改变表面温度的情况下实现电调谐热辐射，如图8(e)所示。此外，自适应热伪装是通过反馈机制实现的。

随着各种探测技术的进步和多样化，多光谱热伪

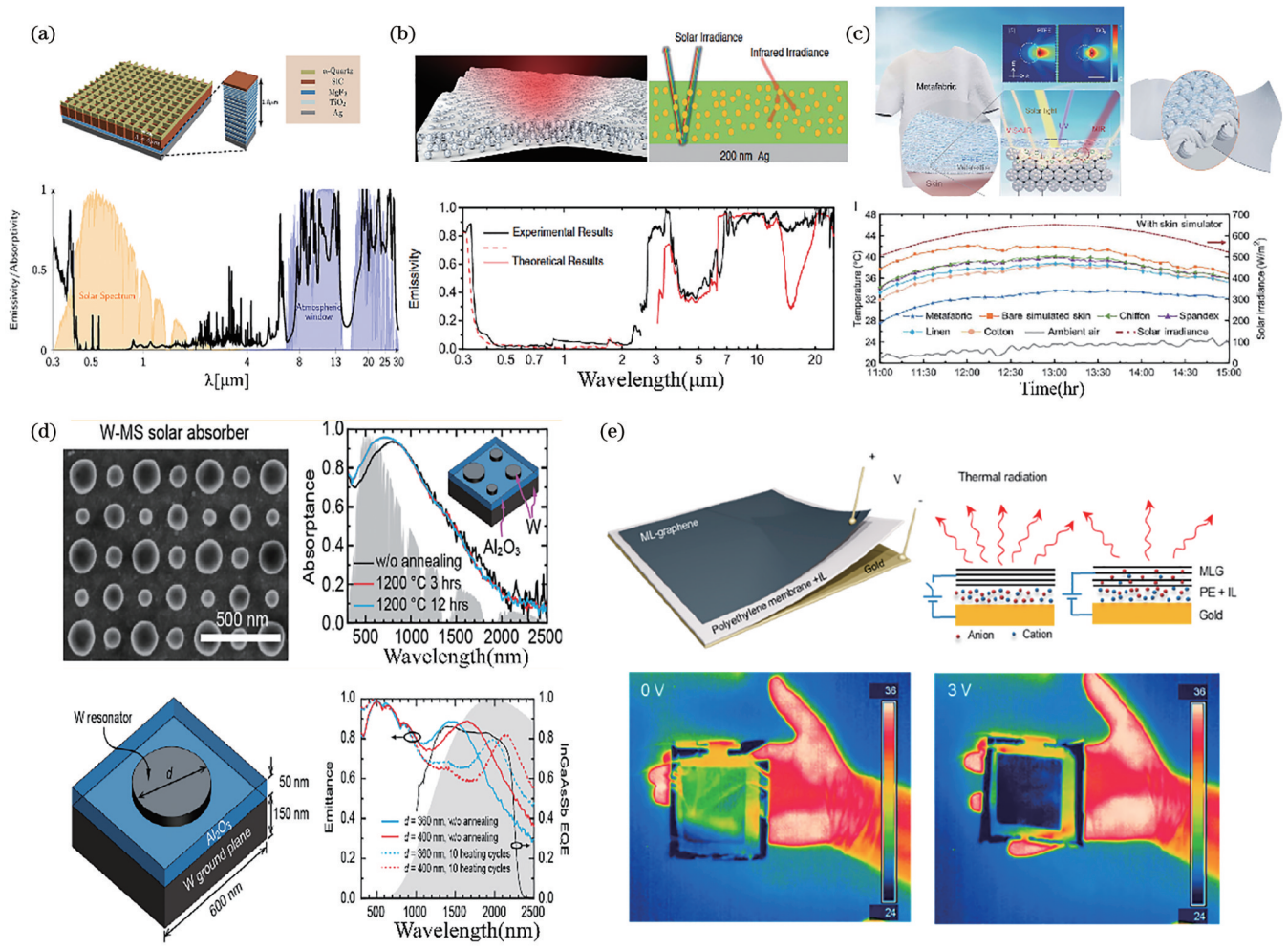

图 8　基于热辐射器件的红外应用。(a)白天辐射制冷器示意图和正入射下的计算辐射率[165];(b)随机分布的 SiO_2 微球包裹体的聚合物掺杂辐射制冷器示意图及实测辐射谱与理论结果的对比[167];(c)日间辐射制冷的超构纺织物示意图(蓝色、绿色和红色虚线框分别突出了响应紫外(UV)、可见光到近红外(VIS-NIR)和中红外(MIR)波段的三级层次结构),以及皮肤模拟器在同一位置不同织物样品下的温差[171];(d)钨超表面太阳能吸收器在退火前和 10 次加热循环后的热稳定性和辐射率[174];(e)基于多层石墨烯的超表面设计、主动热表面的工作原理,以及在 0 V 和 3 V 电压偏置下超表面放置在作者手上的热图像具有热伪装效果[194]

Fig. 8　Infrared applications based on thermal emitters. (a) Schematic of the daytime radiative cooler and calculated emissivity at normal incidence[165]; (b) schematic of the polymer-based hybrid radiative cooler with randomly distributed SiO_2 microsphere inclusions and measured emission spectra of hybrid radiative cooler compared with theoretical results[167]; (c) schematic of a metafabric for daytime radiative cooling (blue, green, and red dashed boxes highlight the three-level hierarchical structure responding to the UV, VIS-NIR, and MIR bands, respectively) and temperature difference of skin simulator under different fabric samples in the same location[171]; (d) thermal stability and emittance of tungsten metasurface solar absorbers before annealing and after 10 heating cycles[174]; (e) multilayer graphene based metasurface design, working principle of active thermal surface, and thermal images of the camouflage design placed on the author's hand under the voltage biases of 0 and 3 V, respectively[194]

装目前已成为研究热点[199]。未来,通过将多光谱设计与活性材料相结合,有望实现具有可切换操作波段的自适应热伪装,从而促进自适应热管理器件的发展。

9　基于超表面阵列的集成热辐射芯片

热辐射在波长、偏振、角度等多个自由度上的调控已经得到了广泛的研究。然而,这些研究大多是在单个超表面结构上进行的,热辐射调控的自由度有限。进一步扩大调控自由度对实际的红外应用至关重要。像素化超表面阵列[14, 43, 206]是解决这一问题的有效方法。将多功能热辐射器集成到单个芯片中,可以进一步促进红外器件的集成化和小型化。

Chu 等[207]通过像素化超构微腔阵列展示了一种辐射波长覆盖 7~9 μm 和 10~14 μm 的热辐射微芯片,如图 9(a)、(c)所示。每个微腔由纳米孔超表面和法布里-珀罗(FP)腔组成,在长波红外范围内具有两个辐射峰,表现出很强的 x 偏振热辐射,如图 9(b)、(d)所示。超构微腔的共振辐射波长随纳米孔孔长的增加向长波方向移动。通过设计将纳米孔排列成“NJU”和

“PHY”图案，可以进一步实现偏振、波长和空间复用的热辐射，热成像结果如图 9(e)所示。这种多路复用现象源于“NJU”和“PHY”的结构参数、空间分布和纳米孔方向的不同。

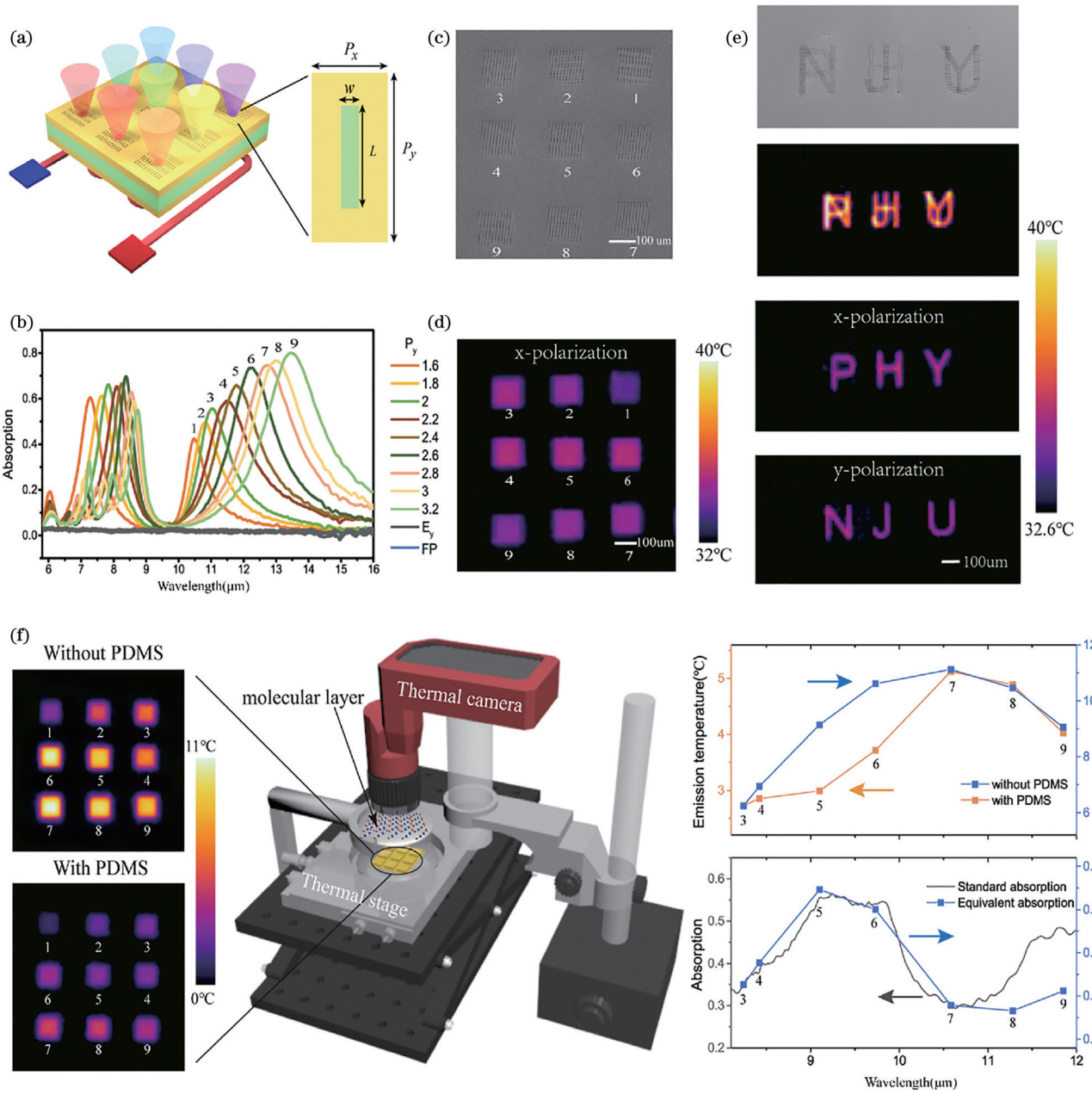

图 9　基于超表面阵列的集成热辐射芯片。(a) 3×3 像素化超构微腔阵列组成的热辐射芯片示意图[207]；超构微腔阵列的(b)实验吸收光谱和(c) SEM 图[207]；(d)超构微腔阵列在 x 偏振下的热像图[207]；(e)制备的“NJU”和“PHY”纳米孔图案的 SEM 图和纳米孔图案的热像图[207]；(f)含 PDMS 层和不含 PDMS 层的超构微腔阵列热像图测量装置，以及测量得到的阵列不同像素的辐射温度和 PDMS 层的等效吸收光谱[208]

Fig. 9　Integrated thermal emission chip based on metasurface array. (a) Schematic of designed thermal emission chip composed of 3×3 meta-cavity array[207]; (b) measured absorption spectra and (c) SEM picture of meta-cavity array[207]; (d) thermal image of meta-cavity array under x polarization[207]; (e) SEM picture of fabricated nanohole patterns of “NJU” and “PHY” and thermal images of nanohole patterns[207]; (f) measurement setup for measurement of thermal images of meta-cavity array with and without PDMS layer, and measured emission temperature of meta-cavity pixels and measured equivalent absorption spectra of PDMS layer[208]

基于这种热辐射芯片设计和热成像方法，Chu 等[208]进一步提出了一种间接吸收光谱测量技术，如图 9(f)所示。与传统的吸收光谱测量方法相比，该测量技术不需要额外的红外辐射光源和复杂的光谱仪装置，具有高度紧凑的特点。前面提到的热辐射芯片可以同时作为探测过程中低成本的红外辐射源和光谱芯片。通过对像素化超构微腔阵列的热成像，可以从空间分布的单个超构微腔中获得被检测样品的等效光谱

吸收信息。这种测量技术的波长分辨率有望通过利用电介质超表面或BIC模式中的共振来提高[209]。所提出的集成化间接吸收光谱测量技术可以促进片上红外光谱的应用,如气体传感器和微型生化传感器。

10 结束语

这篇综述展示了超表面是一个可以精确且灵活多自由度调控热辐射的强大工具。首先,波长选择性热辐射是提高各种热管理应用效率的关键,基于超表面的热辐射器件已经成功获得了许多红外器件所需的辐射光谱。其次,本文还分别讨论了热辐射的辐射方向、偏振和相干特性的灵活调控。此外,还重点回顾了非互易热辐射和近场热辐射的相关内容,非互易热辐射和近场热辐射的深入研究对热光伏器件和传热应用具有重要意义。为了获得更多的可调自由度,在单芯片上集成超表面阵列是一种很有前景的方法。

考虑到集成化与小型化是未来超薄和紧凑型红外应用发展的趋势,片上热辐射调控仍存在几个问题急需解决:1)结合调控机制的多光谱热管理设计(从可见光到长波红外范围)可以进一步集成器件,促进紧凑的多功能红外应用,例如在所要求的波长范围内的选择性隐身,以及从防伪到辐射制冷等多种功能之间的灵活切换;2)高Q热辐射对于红外传感器和探测应用是必不可少的,进一步提高热辐射器件阵列的Q因子可以获得更高的分辨率以满足紧凑光谱应用的商业要求;3)随着人工智能技术的发展,如何快速实现超表面结构的智能化逆向设计也是亟待解决的问题,机器学习为实现特定需求的超表面设计提供了新的途径;4)热辐射方向调控大多存在缺乏动态调控能力的问题以及宽带定向热辐射的角度发散等问题[210],相变材料和将近零介电常数材料与超表面相结合的优化设计有望解决这些问题;5)超表面与红外探测器的集成化仍受制于目前的微纳加工技术,大面积加工面临较高的成本制约[211],未来随着微纳加工技术的进步,可以实现超表面的大面积制备;6)电调控是快速调控热辐射的常用方法。未来,结合超快激光技术(如阿秒激光)的超表面设计可能会将热辐射的调制速度提升到一个新的水平,从而促进各种动态热开关器件的发展。

近年来,通过将拓扑、莫尔和非厄米光子学等光学研究里的特殊物理机制与热辐射调控机制结合到超表面设计中,可以预见各种奇特的红外现象。例如:具有BIC模式的超表面可以在动量空间中提供独特的辐射特性;具有额外转角自由度的莫尔光子设计,可以为转角控制的近场、远场和非互易热辐射带来新的效果。此外,非厄米体系中可以产生奇异点、奇异环甚至特殊的哈密顿量用于调控热辐射。

参 考 文 献

[1] Diem M, Koschny T, Soukoulis C M. Wide-angle perfect absorber/thermal emitter in the terahertz regime[J]. Physical Review B, 2009, 79(3): 033101.

[2] Doiron C F, Naik G V. Non-Hermitian selective thermal emitters using metal-semiconductor hybrid resonators[J]. Advanced Materials, 2019, 31(44): e1904154.

[3] Dyachenko P N, Molesky S, Petrov A Y, et al. Controlling thermal emission with refractory epsilon-near-zero metamaterials via topological transitions[J]. Nature Communications, 2016, 7: 11809.

[4] Xu J, Mandal J, Raman A P. Broadband directional control of thermal emission[J]. Science, 2021, 372(6540): 393-397.

[5] Lin S Y, Moreno J, Fleming J G. Three-dimensional photonic-crystal emitter for thermal photovoltaic power generation[J]. Applied Physics Letters, 2003, 83(2): 380-382.

[6] Arpin K A, Losego M D, Cloud A N, et al. Three-dimensional self-assembled photonic crystals with high temperature stability for thermal emission modification[J]. Nature Communications, 2013, 4: 2630.

[7] Rinnerbauer V, Lenert A, Bierman D M, et al. Metallic photonic crystal absorber-emitter for efficient spectral control in high-temperature solar thermophotovoltaics[J]. Advanced Energy Materials, 2014, 4(12): 1400334.

[8] Liu X X, Li Z W, Wen Z J, et al. Large-area, lithography-free, narrow-band and highly directional thermal emitter[J]. Nanoscale, 2019, 11(42): 19742-19750.

[9] Liu L X, Zhang X Q, Kenney M, et al. Broadband metasurfaces with simultaneous control of phase and amplitude[J]. Advanced Materials, 2014, 26(29): 5031-5036.

[10] Yu N F, Capasso F. Flat optics with designer metasurfaces[J]. Nature Materials, 2014, 13(2): 139-150.

[11] Wang Q, Xiao M, Liu H, et al. Measurement of the Zak phase of photonic bands through the interface states of a metasurface/photonic crystal[J]. Physical Review B, 2016, 93(4): 041415.

[12] Yu N F, Genevet P, Kats M A, et al. Light propagation with phase discontinuities: generalized laws of reflection and refraction [J]. Science, 2011, 334(6054): 333-337.

[13] Gao L H, Cheng Q, Yang J, et al. Broadband diffusion of terahertz waves by multi-bit coding metasurfaces[J]. Light: Science & Applications, 2015, 4(9): e324.

[14] Xiao S Y, Zhong F, Liu H, et al. Flexible coherent control of plasmonic spin-Hall effect[J]. Nature Communications, 2015, 6: 8360.

[15] Maguid E, Yulevich I, Veksler D, et al. Photonic spin-controlled multifunctional shared-aperture antenna array[J]. Science, 2016, 352(6290): 1202-1206.

[16] Qiao T, Hu M Y, Jiang X, et al. Generation and tunability of supermodes in Tamm plasmon topological superlattices[J]. ACS Photonics, 2021, 8(7): 2095-2102.

[17] Liu H, Cao J X, Zhu S N, et al. Lagrange model for the chiral optical properties of stereometamaterials[J]. Physical Review B, 2010, 81(24): 241403.

[18] Arbabi A, Horie Y, Bagheri M, et al. Dielectric metasurfaces for complete control of phase and polarization with subwavelength spatial resolution and high transmission[J]. Nature Nanotechnology, 2015, 10(11): 937-943.

[19] Yang Y M, Wang W Y, Moitra P, et al. Dielectric meta-reflectarray for broadband linear polarization conversion and optical vortex generation[J]. Nano Letters, 2014, 14(3): 1394-1399.

[20] Chen K, Feng Y J, Monticone F, et al. A reconfigurable active Huygens′ metalens[J]. Advanced Materials, 2017, 29(17): 1606422.

[21] Wang S M, Wu P C, Su V C, et al. Broadband achromatic

optical metasurface devices[J]. Nature Communications, 2017, 8: 187.
[22] Neubrech F, Huck C, Weber K, et al. Surface-enhanced infrared spectroscopy using resonant nanoantennas[J]. Chemical Reviews, 2017, 117(7): 5110-5145.
[23] Tittl A, Leitis A, Liu M K, et al. Imaging-based molecular barcoding with pixelated dielectric metasurfaces[J]. Science, 2018, 360(6393): 1105-1109.
[24] Zhu Z H, Liu H, Wang S M, et al. Optically pumped nanolaser based on two magnetic plasmon resonance modes[J]. Applied Physics Letters, 2009, 94(10): 103106.
[25] Hao J M, Wang J, Liu X L, et al. High performance optical absorber based on a plasmonic metamaterial[J]. Applied Physics Letters, 2010, 96(25): 251104.
[26] Liu N, Mesch M, Weiss T, et al. Infrared perfect absorber and its application as plasmonic sensor[J]. Nano Letters, 2010, 10(7): 2342-2348.
[27] Liu H, Ng J, Wang S B, et al. Strong light-induced negative optical pressure arising from kinetic energy of conduction electrons in plasmon-type cavities[J]. Physical Review Letters, 2011, 106(8): 087401.
[28] Liu H, Li G X, Li K F, et al. Linear and nonlinear Fano resonance on two-dimensional magnetic metamaterials[J]. Physical Review B, 2011, 84(23): 235437.
[29] Landy N I, Sajuyigbe S, Mock J J, et al. Perfect metamaterial absorber[J]. Physical Review Letters, 2008, 100(20): 207402.
[30] Chen H T. Interference theory of metamaterial perfect absorbers [J]. Optics Express, 2012, 20(7): 7165-7172.
[31] Chen K, Adato R, Altug H. Dual-band perfect absorber for multispectral plasmon-enhanced infrared spectroscopy[J]. ACS Nano, 2012, 6(9): 7998-8006.
[32] Li W, Valentine J. Metamaterial perfect absorber based hot electron photodetection[J]. Nano Letters, 2014, 14(6): 3510-3514.
[33] Wang C M, Chang Y C, Tsai M W, et al. Reflection and emission properties of an infrared emitter[J]. Optics Express, 2007, 15(22): 14673-14678.
[34] Park S J, Kim Y B, Moon Y J, et al. Tuning of polarized room-temperature thermal radiation based on nanogap plasmon resonance[J]. Optics Express, 2020, 28(10): 15472-15481.
[35] Ikeda K, Miyazaki H T, Kasaya T, et al. Controlled thermal emission of polarized infrared waves from arrayed plasmon nanocavities[J]. Applied Physics Letters, 2008, 92(2): 021117.
[36] Liu Z, Shimizu M, Yugami H. Emission bandwidth control on a two-dimensional superlattice microcavity array[J]. Optics Express, 2022, 30(8): 13839-13846.
[37] Zhu L X, Sandhu S, Otey C, et al. Temporal coupled mode theory for thermal emission from a single thermal emitter supporting either a single mode or an orthogonal set of modes[J]. Applied Physics Letters, 2013, 102(10): 103104.
[38] Woolf D, Hensley J, Cederberg J G, et al. Heterogeneous metasurface for high temperature selective emission[J]. Applied Physics Letters, 2014, 105(8): 081110.
[39] Asano T, Suemitsu M, Hashimoto K, et al. Near-infrared-to-visible highly selective thermal emitters based on an intrinsic semiconductor[J]. Science Advances, 2016, 2(12): e1600499.
[40] Howes A, Nolen J R, Caldwell J D, et al. Near-unity and narrowband thermal emissivity in balanced dielectric metasurfaces[J]. Advanced Optical Materials, 2020, 8(4): 1901470.
[41] Li J Y, Yu B W, Shen S. Scale law of far-field thermal radiation from plasmonic metasurfaces[J]. Physical Review Letters, 2020, 124(13): 137401.
[42] Kudyshev Z A, Kildishev A V, Shalaev V M, et al. Machine-learning-assisted metasurface design for high-efficiency thermal emitter optimization[J]. Applied Physics Reviews, 2020, 7(2): 021407.
[43] Makhsiyan M, Bouchon P, Jaeck J, et al. Shaping the spatial and spectral emissivity at the diffraction limit[J]. Applied Physics Letters, 2015, 107(25): 251103.
[44] Streyer W, Feng K, Zhong Y, et al. Selective absorbers and thermal emitters for far-infrared wavelengths[J]. Applied Physics Letters, 2015, 107(8): 081105.
[45] Matsuno Y, Sakurai A. Perfect infrared absorber and emitter based on a large-area metasurface[J]. Optical Materials Express, 2017, 7(2): 618-626.
[46] Lochbaum A, Fedoryshyn Y, Dorodnyy A, et al. On-chip narrowband thermal emitter for mid-IR optical gas sensing[J]. ACS Photonics, 2017, 4(6): 1371-1380.
[47] Liu X L, Tyler T, Starr T, et al. Taming the blackbody with infrared metamaterials as selective thermal emitters[J]. Physical Review Letters, 2011, 107(4): 045901.
[48] de Zoysa M, Asano T, Mochizuki K, et al. Conversion of broadband to narrowband thermal emission through energy recycling[J]. Nature Photonics, 2012, 6: 535-539.
[49] Argyropoulos C, Le K Q, Mattiucci N, et al. Broadband absorbers and selective emitters based on plasmonic Brewster metasurfaces[J]. Physical Review B, 2013, 87(20): 205112.
[50] Hossain M M, Jia B H, Gu M. A metamaterial emitter for highly efficient radiative cooling[J]. Advanced Optical Materials, 2015, 3(8): 1047-1051.
[51] Kong A R, Cai B Y, Shi P, et al. Ultra-broadband all-dielectric metamaterial thermal emitter for passive radiative cooling[J]. Optics Express, 2019, 27(21): 30102-30115.
[52] Liu G Q, Liu X S, Chen J, et al. Near-unity, full-spectrum, nanoscale solar absorbers and near-perfect blackbody emitters[J]. Solar Energy Materials and Solar Cells, 2019, 190: 20-29.
[53] Zou C J, Ren G H, Hossain M M, et al. Metal-loaded dielectric resonator metasurfaces for radiative cooling[J]. Advanced Optical Materials, 2017, 5(20): 1700460.
[54] Song J, Seo J, Han J, et al. Ultrahigh emissivity of grating-patterned PDMS film from 8 to 13 μm wavelength regime[J]. Applied Physics Letters, 2020, 117(9): 094101.
[55] Xu C L, Qu S B, Pang Y Q, et al. Metamaterial absorber for frequency selective thermal radiation[J]. Infrared Physics & Technology, 2018, 88: 133-138.
[56] Cao T, Lian M, Liu K, et al. Wideband mid-infrared thermal emitter based on stacked nanocavity metasurfaces[J]. International Journal of Extreme Manufacturing, 2022, 4(1): 015402.
[57] Chen C, Liu Y H, Jiang Z Y, et al. Large-area long-wave infrared broadband all-dielectric metasurface absorber based on markless laser direct writing lithography[J]. Optics Express, 2022, 30(8): 13391-13403.
[58] Zhu Y, Hou G Z, Wang Q Y, et al. Silicon-based spectrally selective emitters with good high-temperature stability on stepped metasurfaces[J]. Nanoscale, 2022, 14(30): 10816-10822.
[59] Zhou J R, Zhan Z G, Zhu F D, et al. Preparation of flexible wavelength-selective metasurface for infrared radiation regulation [J]. ACS Applied Materials & Interfaces, 2023, 15(17): 21629-21639.
[60] Schuller J A, Taubner T, Brongersma M L. Optical antenna thermal emitters[J]. Nature Photonics, 2009, 3: 658-661.
[61] Liu B A, Gong W, Yu B W, et al. Perfect thermal emission by nanoscale transmission line resonators[J]. Nano Letters, 2017, 17(2): 666-672.
[62] Dahan N, Niv A, Biener G, et al. Space-variant polarization manipulation of a thermal emission by a SiO_2 subwavelength grating supporting surface phonon-polaritons[J]. Applied Physics Letters, 2005, 86(19): 191102.
[63] Mason J A, Smith S, Wasserman D. Strong absorption and selective thermal emission from a midinfrared metamaterial[J]. Applied Physics Letters, 2011, 98(24): 241105.

[64] Shitrit N, Yulevich I, Maguid E, et al. Spin-optical metamaterial route to spin-controlled photonics[J]. Science, 2013, 340(6133): 724-726.
[65] Khandekar C, Jacob Z. Circularly polarized thermal radiation from nonequilibrium coupled antennas[J]. Physical Review Applied, 2019, 12(1): 014053.
[66] Gao W L, Doiron C F, Li X W, et al. Macroscopically aligned carbon nanotubes as a refractory platform for hyperbolic thermal emitters[J]. ACS Photonics, 2019, 6(7): 1602-1609.
[67] Dahan N, Gorodetski Y, Frischwasser K, et al. Geometric Doppler effect: spin-split dispersion of thermal radiation[J]. Physical Review Letters, 2010, 105(13): 136402.
[68] Dyakov S A, Semenenko V A, Gippius N A, et al. Magnetic field free circularly polarized thermal emission from a chiral metasurface[J]. Physical Review B, 2018, 98(23): 235416.
[69] Ginn J, Shelton D, Krenz P, et al. Polarized infrared emission using frequency selective surfaces[J]. Optics Express, 2010, 18(5): 4557-4563.
[70] Nguyen A, Hugonin J P, Coutrot A L, et al. Large circular dichroism in the emission from an incandescent metasurface[J]. Optica, 2023, 10(2): 232-238.
[71] Wang X J, Sentz T, Bharadwaj S, et al. Observation of nonvanishing optical helicity in thermal radiation from symmetry-broken metasurfaces[J]. Science Advances, 2023, 9(4): eade4203.
[72] Dahan N, Niv A, Biener G, et al. Enhanced coherency of thermal emission: beyond the limitation imposed by delocalized surface waves[J]. Physical Review B, 2007, 76(4): 045427.
[73] Arnold C, Marquier F, Garin M, et al. Coherent thermal infrared emission by two-dimensional silicon carbide gratings[J]. Physical Review B, 2012, 86(3): 035316.
[74] Lu G Y, Tadjer M, Caldwell J D, et al. Multi-frequency coherent emission from superstructure thermal emitters[J]. Applied Physics Letters, 2021, 118(14): 141102.
[75] Liu J J, Guler U, Lagutchev A, et al. Quasi-coherent thermal emitter based on refractory plasmonic materials[J]. Optical Materials Express, 2015, 5(12): 2721-2728.
[76] Liao C Y, Wang C M, Cheng B H, et al. Quasi-coherent thermal radiation with multiple resonant plasmonic cavities[J]. Applied Physics Letters, 2016, 109(26): 261101.
[77] Greffet J J, Carminati R, Joulain K, et al. Coherent emission of light by thermal sources[J]. Nature, 2002, 416(6876): 61-64.
[78] Lee B J, Wang L P, Zhang Z M. Coherent thermal emission by excitation of magnetic polaritons between periodic strips and a metallic film[J]. Optics Express, 2008, 16(15): 11328-11336.
[79] Sun K L, Levy U, Han Z H. Thermal emission with high temporal and spatial coherence by harnessing quasiguided modes [J]. Physical Review Applied, 2023, 20(2): 024033.
[80] Yu J B, Qin R, Ying Y B, et al. Asymmetric directional control of thermal emission[J]. Advanced Materials, 2023, 35(45): 2302478.
[81] Biener G, Dahan N, Niv A, et al. Highly coherent thermal emission obtained by plasmonic bandgap structures[J]. Applied Physics Letters, 2008, 92(8): 081913.
[82] Yang Y, Taylor S, Alshehri H, et al. Wavelength-selective and diffuse infrared thermal emission mediated by magnetic polaritons from silicon carbide metasurfaces[J]. Applied Physics Letters, 2017, 111(5): 051904.
[83] Han S E, Norris D J. Beaming thermal emission from hot metallic bull's eyes[J]. Optics Express, 2010, 18(5): 4829-4837.
[84] Park J H, Han S E, Nagpal P, et al. Observation of thermal beaming from tungsten and molybdenum bull's eyes[J]. ACS Photonics, 2016, 3(3): 494-500.
[85] Costantini D, Lefebvre A, Coutrot A L, et al. Plasmonic metasurface for directional and frequency-selective thermal emission[J]. Physical Review Applied, 2015, 4(1): 014023.
[86] Overvig A C, Mann S A, Alù A. Thermal metasurfaces: complete emission control by combining local and nonlocal light-matter interactions[J]. Physical Review X, 2021, 11(2): 021050.
[87] Chalabi H, Alù A, Brongersma M L. Focused thermal emission from a nanostructured SiC surface[J]. Physical Review B, 2016, 94(9): 094307.
[88] Zhou M, Khoram E, Liu D J, et al. Self-focused thermal emission and holography realized by mesoscopic thermal emitters [J]. ACS Photonics, 2021, 8(2): 497-504.
[89] Wang T, Li P N, Chigrin D N, et al. Phonon-polaritonic bowtie nanoantennas: controlling infrared thermal radiation at the nanoscale[J]. ACS Photonics, 2017, 4(7): 1753-1760.
[90] Lee G J, Kim D H, Heo S Y, et al. Spectrally and spatially selective emitters using polymer hybrid spoof plasmonics[J]. ACS Applied Materials & Interfaces, 2020, 12(47): 53206-53214.
[91] Audhkhasi R, Zhao B, Fan S H, et al. Spectral emissivity modeling in multi-resonant systems using coupled-mode theory [J]. Optics Express, 2022, 30(6): 9463-9472.
[92] Nishijima Y, Morimoto S, Balčytis A, et al. Coupling of molecular vibration and metasurface modes for efficient mid-infrared emission[J]. Journal of Materials Chemistry C, 2022, 10(2): 451-462.
[93] Zhang X, Liu H, Zhang Z G, et al. Controlling thermal emission of phonon by magnetic metasurfaces[J]. Scientific Reports, 2017, 7: 41858.
[94] Zhang X, Zhang Z G, Wang Q, et al. Controlling thermal emission by parity-symmetric Fano resonance of optical absorbers in metasurfaces[J]. ACS Photonics, 2019, 6(11): 2671-2676.
[95] Zhong F, Ding K, Zhang Y, et al. Angle-resolved thermal emission spectroscopy characterization of non-Hermitian metacrystals[J]. Physical Review Applied, 2020, 13(1): 014071.
[96] Zhong F, Zhang Y, Zhu S N, et al. Probing mid-infrared surface interface states based on thermal emission[J]. Optics Express, 2021, 29(22): 35216-35225.
[97] Freitag M, Chiu H Y, Steiner M, et al. Thermal infrared emission from biased graphene[J]. Nature Nanotechnology, 2010, 5(7): 497-501.
[98] Brar V W, Sherrott M C, Jang M S, et al. Electronic modulation of infrared radiation in graphene plasmonic resonators [J]. Nature Communications, 2015, 6: 7032.
[99] Luo F, Fan Y S, Peng G, et al. Graphene thermal emitter with enhanced joule heating and localized light emission in air[J]. ACS Photonics, 2019, 6(8): 2117-2125.
[100] Li Y Y, Ferreyra P, Swan A K, et al. Current-driven terahertz light emission from graphene plasmonic oscillations[J]. ACS Photonics, 2019, 6(10): 2562-2569.
[101] Zhang Y M, Antezza M, Wang J S. Controllable thermal radiation from twisted bilayer graphene[J]. International Journal of Heat and Mass Transfer, 2022, 194: 123076.
[102] Shi C, Mahlmeister N H, Luxmoore I J, et al. Metamaterial-based graphene thermal emitter[J]. Nano Research, 2018, 11(7): 3567-3573.
[103] Shiue R J, Gao Y D, Tan C, et al. Thermal radiation control from hot graphene electrons coupled to a photonic crystal nanocavity[J]. Nature Communications, 2019, 10: 109.
[104] Yuan H, Zhang H, Huang K W, et al. Dual-emitter graphene glass fiber fabric for radiant heating[J]. ACS Nano, 2022, 16(2): 2577-2584.
[105] Park J, Kang J H, Liu X G, et al. Dynamic thermal emission control with InAs-based plasmonic metasurfaces[J]. Science Advances, 2018, 4(12): eaat3163.
[106] Inoue T, de Zoysa M, Asano T, et al. Realization of dynamic thermal emission control[J]. Nature Materials, 2014, 13(10): 928-931.
[107] Kang D D, Inoue T, Asano T, et al. Electrical modulation of narrowband GaN/AlGaN quantum-well photonic crystal thermal

emitters in mid-wavelength infrared[J]. ACS Photonics, 2019, 6(6): 1565-1571.
[108] Wu S H, Chen M K, Barako M T, et al. Thermal homeostasis using microstructured phase-change materials[J]. Optica, 2017, 4(11): 1390-1396.
[109] Chandra S, Franklin D, Cozart J, et al. Adaptive multispectral infrared camouflage[J]. ACS Photonics, 2018, 5(11): 4513-4519.
[110] Ito K, Watari T, Nishikawa K, et al. Inverting the thermal radiative contrast of vanadium dioxide by metasurfaces based on localized gap-plasmons[J]. APL Photonics, 2018, 3(8): 086101.
[111] Long L S, Taylor S, Wang L P. Enhanced infrared emission by thermally switching the excitation of magnetic polariton with scalable microstructured VO_2 metasurfaces[J]. ACS Photonics, 2020, 7(8): 2219-2227.
[112] Sun K, Xiao W, Wheeler C, et al. VO_2 metasurface smart thermal emitter with high visual transparency for passive radiative cooling regulation in space and terrestrial applications[J]. Nanophotonics, 2022, 11(17): 4101-4114.
[113] Qu Y R, Li Q, Du K K, et al. Dynamic thermal emission control based on ultrathin plasmonic metamaterials including phase-changing material GST[J]. Laser & Photonics Reviews, 2017, 11(5): 1700091.
[114] Cao T, Zhang X Y, Dong W L, et al. Tuneable thermal emission using chalcogenide metasurface[J]. Advanced Optical Materials, 2018, 6(16): 1800169.
[115] Li S C, Simpson R E, Shin S. Enhanced far-field coherent thermal emission using mid-infrared bilayer metasurfaces[J]. Nanoscale, 2023, 15(39): 15965-15974.
[116] Khalichi B, Ghobadi A, Osgouei A K, et al. Phase-change Fano resonator for active modulation of thermal emission[J]. Nanoscale, 2023, 15(25): 10783-10793.
[117] Conrads L, Honné N, Ulm A, et al. Reconfigurable and polarization-dependent grating absorber for large-area emissivity control based on the plasmonic phase-change material In_3SbTe_2[J]. Advanced Optical Materials, 2023, 11(8): 2202696.
[118] Roberts J A, Ho P H, Yu S J, et al. Electrically driven hyperbolic nanophotonic resonators as high speed, spectrally selective thermal radiators[J]. Nano Letters, 2022, 22(14): 5832-5840.
[119] Li J Y, Li Z, Liu X, et al. Active control of thermal emission by graphene-nanowire coupled plasmonic metasurfaces[J]. Physical Review B, 2022, 106(11): 115416.
[120] Miyoshi Y, Fukazawa Y, Amasaka Y, et al. High-speed and on-chip graphene blackbody emitters for optical communications by remote heat transfer[J]. Nature Communications, 2018, 9: 1279.
[121] Xu Z Q, Li Q, Du K K, et al. Spatially resolved dynamically reconfigurable multilevel control of thermal emission[J]. Laser & Photonics Reviews, 2020, 14(1): 1900162.
[122] Sun R Z, Zhou P H, Ai W S, et al. Broadband switching of mid-infrared atmospheric windows by VO_2-based thermal emitter[J]. Optics Express, 2019, 27(8): 11537-11546.
[123] Liu X Y, Padilla W J. Reconfigurable room temperature metamaterial infrared emitter[J]. Optica, 2017, 4(4): 430-433.
[124] Coppens Z J, Valentine J G. Spatial and temporal modulation of thermal emission[J]. Advanced Materials, 2017, 29(39): 1701275.
[125] Kim C, Kim Y, Kang D, et al. Laser-printed emissive metasurface as an anticounterfeiting platform[J]. Laser & Photonics Reviews, 2022, 16(10): 2200215.
[126] Xu Z Q, Luo H, Zhu H Z, et al. Nonvolatile optically reconfigurable radiative metasurface with visible tunability for anticounterfeiting[J]. Nano Letters, 2021, 21(12): 5269-5276.
[127] Tsurimaki Y, Qian X, Pajovic S, et al. Large nonreciprocal absorption and emission of radiation in type-I Weyl semimetals with time reversal symmetry breaking[J]. Physical Review B, 2020, 101(16): 165426.
[128] Shayegan K J, Zhao B, Kim Y, et al. Nonreciprocal infrared absorption via resonant magneto-optical coupling to InAs[J]. Science Advances, 2022, 8(18): eabm4308.
[129] Wu J, Wu F, Zhao T C, et al. Tunable nonreciprocal thermal emitter based on metal grating and graphene[J]. International Journal of Thermal Sciences, 2022, 172: 107316.
[130] Zhang Z N, Zhu L X. Nonreciprocal thermal photonics for energy conversion and radiative heat transfer[J]. Physical Review Applied, 2022, 18(2): 027001.
[131] Zhao B, Wang J H, Zhao Z X, et al. Nonreciprocal thermal emitters using metasurfaces with multiple diffraction channels[J]. Physical Review Applied, 2021, 16(6): 064001.
[132] Guo C, Zhao B, Fan S H. Adjoint Kirchhoff's law and general symmetry implications for all thermal emitters[J]. Physical Review X, 2022, 12(2): 021023.
[133] Zhu L X, Fan S H. Near complete violation of detailed balance in thermal radiation[J]. Physical Review B, 2014, 90(22): 220301.
[134] Zhao B, Shi Y, Wang J H, et al. Near-complete violation of Kirchhoff's law of thermal radiation with a 0.3 T magnetic field[J]. Optics Letters, 2019, 44(17): 4203-4206.
[135] Zhao B, Guo C, Garcia C A C, et al. Axion-field-enabled nonreciprocal thermal radiation in Weyl semimetals[J]. Nano Letters, 2020, 20(3): 1923-1927.
[136] Park Y, Asadchy V S, Zhao B, et al. Violating Kirchhoff's law of thermal radiation in semitransparent structures[J]. ACS Photonics, 2021, 8(8): 2417-2424.
[137] Hadad Y, Soric J C, Alu A. Breaking temporal symmetries for emission and absorption[J]. Proceedings of the National Academy of Sciences of the United States of America, 2016, 113(13): 3471-3475.
[138] Ghanekar A, Wang J H, Fan S H, et al. Violation of Kirchhoff's law of thermal radiation with space-time modulated grating[J]. ACS Photonics, 2022, 9(4): 1157-1164.
[139] Ghanekar A, Wang J H, Guo C, et al. Nonreciprocal thermal emission using spatiotemporal modulation of graphene[J]. ACS Photonics, 2023, 10(1): 170-178.
[140] Shayegan K J, Biswas S, Zhao B, et al. Direct observation of the violation of Kirchhoff's law of thermal radiation[J]. Nature Photonics, 2023, 17: 891-896.
[141] Khandekar C, Messina R, Rodriguez A W. Near-field refrigeration and tunable heat exchange through four-wave mixing[J]. AIP Advances, 2018, 8(5): 055029.
[142] Khandekar C, Yang L P, Rodriguez A W, et al. Quantum nonlinear mixing of thermal photons to surpass the blackbody limit[J]. Optics Express, 2020, 28(2): 2045-2059.
[143] Cuevas J C, García-Vidal F J. Radiative heat transfer[J]. ACS Photonics, 2018, 5(10): 3896-3915.
[144] Xiao Y Z, Sheldon M, Kats M A. Super-Planckian emission cannot really be 'thermal'[J]. Nature Photonics, 2022, 16(6): 397-401.
[145] Rodriguez A W, Ilic O, Bermel P, et al. Frequency-selective near-field radiative heat transfer between photonic crystal slabs: a computational approach for arbitrary geometries and materials[J]. Physical Review Letters, 2011, 107(11): 114302.
[146] Guérout R, Lussange J, Rosa F S S, et al. Enhanced radiative heat transfer between nanostructured gold plates[J]. Physical Review B, 2012, 85(18): 180301.
[147] Dai J, Dyakov S A, Yan M. Enhanced near-field radiative heat transfer between corrugated metal plates: role of spoof surface plasmon polaritons[J]. Physical Review B, 2015, 92(3): 035419.
[148] Ghanekar A, Ji J, Zheng Y. High-rectification near-field thermal diode using phase change periodic nanostructure[J]. Applied Physics Letters, 2016, 109(12): 123106.
[149] Yang Y, Wang L P. Spectrally enhancing near-field radiative transfer between metallic gratings by exciting magnetic polaritons in nanometric vacuum gaps[J]. Physical Review Letters, 2016, 117(4): 044301.

[150] Messina R, Noto A, Guizal B, et al. Radiative heat transfer between metallic gratings using Fourier modal method with adaptive spatial resolution[J]. Physical Review B, 2017, 95(12): 125404.
[151] Liu X L, Zhang Z M. Near-field thermal radiation between metasurfaces[J]. ACS Photonics, 2015, 2(9): 1320-1326.
[152] Fernández-Hurtado V, García-Vidal F J, Fan S H, et al. Enhancing near-field radiative heat transfer with Si-based metasurfaces[J]. Physical Review Letters, 2017, 118(20): 203901.
[153] Gomez-Diaz J S, Alù A. Flatland optics with hyperbolic metasurfaces[J]. ACS Photonics, 2016, 3(12): 2211-2224.
[154] Zhao B, Guizal B, Zhang Z M, et al. Near-field heat transfer between graphene/hBN multilayers[J]. Physical Review B, 2017, 95(24): 245437.
[155] Shi K Z, Bao F L, He S L. Enhanced near-field thermal radiation based on multilayer graphene-hBN heterostructures[J]. ACS Photonics, 2017, 4(4): 971-978.
[156] Zhang Y, Antezza M, Yi H L, et al. Metasurface-mediated anisotropic radiative heat transfer between nanoparticles[J]. Physical Review B, 2019, 100(8): 085426.
[157] Lim M, Lee S S, Lee B J. Near-field thermal radiation between graphene-covered doped silicon plates[J]. Optics Express, 2013, 21(19): 22173-22185.
[158] Ilic O, Thomas N H, Christensen T, et al. Active radiative thermal switching with graphene plasmon resonators[J]. ACS Nano, 2018, 12(3): 2474-2481.
[159] Tang G M, Zhang L, Zhang Y, et al. Near-field energy transfer between graphene and magneto-optic media[J]. Physical Review Letters, 2021, 127(24): 247401.
[160] Kajihara Y, Kosaka K, Komiyama S. Thermally excited near-field radiation and far-field interference[J]. Optics Express, 2011, 19(8): 7695-7704.
[161] Zare S, Pouria R, Chow P K, et al. Probing near-field thermal emission of localized surface phonons from silicon carbide nanopillars[J]. ACS Photonics, 2023, 10(2): 401-411.
[162] St-Gelais R, Zhu L X, Fan S H, et al. Near-field radiative heat transfer between parallel structures in the deep subwavelength regime[J]. Nature Nanotechnology, 2016, 11: 515-519.
[163] Yang J, Du W, Su Y S, et al. Observing of the super-Planckian near-field thermal radiation between graphene sheets[J]. Nature Communications, 2018, 9: 4033.
[164] Bhatt G R, Zhao B, Roberts S, et al. Integrated near-field thermo-photovoltaics for heat recycling[J]. Nature Communications, 2020, 11: 2545.
[165] Rephaeli E, Raman A, Fan S H. Ultrabroadband photonic structures to achieve high-performance daytime radiative cooling [J]. Nano Letters, 2013, 13(4): 1457-1461.
[166] Raman A P, Abou Anoma M, Zhu L X, et al. Passive radiative cooling below ambient air temperature under direct sunlight[J]. Nature, 2014, 515(7528): 540-544.
[167] Zhai Y, Ma Y G, David S N, et al. Scalable-manufactured randomized glass-polymer hybrid metamaterial for daytime radiative cooling[J]. Science, 2017, 355(6329): 1062-1066.
[168] Sun K, Riedel C A, Wang Y D, et al. Metasurface optical solar reflectors using AZO transparent conducting oxides for radiative cooling of spacecraft[J]. ACS Photonics, 2018, 5(2): 495-501.
[169] Salary M M, Mosallaei H. Photonic metasurfaces as relativistic light sails for Doppler-broadened stable beam-riding and radiative cooling[J]. Laser & Photonics Reviews, 2020, 14(8): 1900311.
[170] Li D, Liu X, Li W, et al. Scalable and hierarchically designed polymer film as a selective thermal emitter for high-performance all-day radiative cooling[J]. Nature Nanotechnology, 2021, 16 (2): 153-158.
[171] Zeng S N, Pian S J, Su M Y, et al. Hierarchical-morphology metafabric for scalable passive daytime radiative cooling[J]. Science, 2021, 373(6555): 692-696.
[172] Lin C J, Li Y, Chi C, et al. A solution-processed inorganic emitter with high spectral selectivity for efficient subambient radiative cooling in hot humid climates[J]. Advanced Materials, 2022, 34(12): 2109350.
[173] Zhu Y N, Zhou Y W, Qin B, et al. Night-time radiative warming using the atmosphere[J]. Light: Science & Applications, 2023, 12(1): 268.
[174] Chang C C, Kort-Kamp W J M, Nogan J, et al. High-temperature refractory metasurfaces for solar thermophotovoltaic energy harvesting[J]. Nano Letters, 2018, 18(12): 7665-7673.
[175] Rephaeli E, Fan S H. Absorber and emitter for solar thermo-photovoltaic systems to achieve efficiency exceeding the Shockley-Queisser limit[J]. Optics Express, 2009, 17(17): 15145-15159.
[176] Nguyen-Huu N, Chen Y B, Lo Y L. Development of a polarization-insensitive thermophotovoltaic emitter with a binary grating[J]. Optics Express, 2012, 20(6): 5882-5890.
[177] Wang L P, Zhang Z M. Wavelength-selective and diffuse emitter enhanced by magnetic polaritons for thermophotovoltaics [J]. Applied Physics Letters, 2012, 100(6): 063902.
[178] Wu C H, Neuner B, John J, et al. Metamaterial-based integrated plasmonic absorber/emitter for solar thermo-photovoltaic systems[J]. Journal of Optics, 2012, 14(2): 024005.
[179] Zhao B, Wang L P, Shuai Y, et al. Thermophotovoltaic emitters based on a two-dimensional grating/thin-film nanostructure[J]. International Journal of Heat and Mass Transfer, 2013, 67: 637-645.
[180] Shemelya C, DeMeo D, Latham N P, et al. Stable high temperature metamaterial emitters for thermophotovoltaic applications[J]. Applied Physics Letters, 2014, 104(20): 201113.
[181] Wang H C, Chen Q, Wen L, et al. Titanium-nitride-based integrated plasmonic absorber/emitter for solar thermophotovoltaic application[J]. Photonics Research, 2015, 3 (6): 329-334.
[182] Coppens Z J, Kravchenko I I, Valentine J G. Lithography-free large-area metamaterials for stable thermophotovoltaic energy conversion[J]. Advanced Optical Materials, 2016, 4(5): 671-676.
[183] Wang H, Chang J Y, Yang Y, et al. Performance analysis of solar thermophotovoltaic conversion enhanced by selective metamaterial absorbers and emitters[J]. International Journal of Heat and Mass Transfer, 2016, 98: 788-798.
[184] Woolf D N, Kadlec E A, Bethke D, et al. High-efficiency thermophotovoltaic energy conversion enabled by a metamaterial selective emitter[J]. Optica, 2018, 5(2): 213-218.
[185] Abbas M A, Kim J, Rana A S, et al. Nanostructured chromium-based broadband absorbers and emitters to realize thermally stable solar thermophotovoltaic systems[J]. Nanoscale, 2022, 14 (17): 6425-6436.
[186] Zhang S Y, Zhong F, Lin Z H, et al. Spectrum-selective high-temperature tolerant thermal emitter by dual-coherence enhanced absorption for solar thermophotovoltaics[J]. Advanced Optical Materials, 2024, 12(5): 2301726.
[187] Miyazaki H T, Kasaya T, Iwanaga M, et al. Dual-band infrared metasurface thermal emitter for CO_2 sensing[J]. Applied Physics Letters, 2014, 105(12): 121107.
[188] Pusch A, de Luca A, Oh S S, et al. A highly efficient CMOS nanoplasmonic crystal enhanced slow-wave thermal emitter improves infrared gas-sensing devices[J]. Scientific Reports, 2015, 5: 17451.
[189] Lochbaum A, Dorodnyy A, Koch U, et al. Compact mid-infrared gas sensing enabled by an all-metamaterial design[J]. Nano Letters, 2020, 20(6): 4169-4176.
[190] Li N X, Yuan H Y, Xu L F, et al. Tailorable infrared emission of microelectromechanical system-based thermal emitters with NiO films for gas sensing[J]. Optics Express, 2021, 29(12): 19084-19093.

[191] Livingood A, Nolen J R, Folland T G, et al. Filterless nondispersive infrared sensing using narrowband infrared emitting metamaterials[J]. ACS Photonics, 2021, 8(2): 472-480.
[192] Barho F B, Gonzalez-Posada F, Bomers M, et al. Surface-enhanced thermal emission spectroscopy with perfect absorber metasurfaces[J]. ACS Photonics, 2019, 6(6): 1506-1514.
[193] Nakagawa K, Shimura Y, Fukazawa Y, et al. Microemitter-based IR spectroscopy and imaging with multilayer graphene thermal emission[J]. Nano Letters, 2022, 22(8): 3236-3244.
[194] Salihoglu O, Uzlu H B, Yakar O, et al. Graphene-based adaptive thermal camouflage[J]. Nano Letters, 2018, 18(7): 4541-4548.
[195] Xie X, Li X, Pu M B, et al. Plasmonic metasurfaces for simultaneous thermal infrared invisibility and holographic illusion[J]. Advanced Functional Materials, 2018, 28(14): 1706673.
[196] Lee N, Kim T, Lim J S, et al. Metamaterial-selective emitter for maximizing infrared camouflage performance with energy dissipation[J]. ACS Applied Materials & Interfaces, 2019, 11(23): 21250-21257.
[197] Liu Y D, Song J L, Zhao W X, et al. Dynamic thermal camouflage via a liquid-crystal-based radiative metasurface[J]. Nanophotonics, 2020, 9(4): 855-863.
[198] Song J L, Huang S Y, Ma Y P, et al. Radiative metasurface for thermal camouflage, illusion and messaging[J]. Optics Express, 2020, 28(2): 875-885.
[199] Wang J, Yang F B, Xu L J, et al. Omnithermal restructurable metasurfaces for both infrared-light illusion and visible-light similarity[J]. Physical Review Applied, 2020, 14(1): 014008.
[200] Zhu H Z, Li Q, Tao C N, et al. Multispectral camouflage for infrared, visible, lasers and microwave with radiative cooling[J]. Nature Communications, 2021, 12: 1805.
[201] Kim J, Park C, Hahn J W. Metal-semiconductor-metal metasurface for multiband infrared stealth technology using camouflage color pattern in visible range[J]. Advanced Optical Materials, 2022, 10(6): 2101930.
[202] Wu Y J, Luo J, Pu M B, et al. Optically transparent infrared selective emitter for visible-infrared compatible camouflage[J]. Optics Express, 2022, 30(10): 17259-17269.
[203] Zhang J G, Wen Z J, Zhou Z J, et al. Long-wavelength infrared selective emitter for thermal infrared camouflage under a hot environment[J]. Optics Express, 2022, 30(13): 24132-24144.
[204] Lee N, Lim J S, Chang I, et al. Flexible assembled metamaterials for infrared and microwave camouflage[J]. Advanced Optical Materials, 2022, 10(11): 2200448.
[205] Shim H B, Han K, Song J, et al. A multispectral single-layer frequency selective surface absorber for infrared and millimeter wave selective bi-stealth[J]. Advanced Optical Materials, 2022, 10(6): 2102107.
[206] Qin B, Zhu Y N, Zhou Y W, et al. Whole-infrared-band camouflage with dual-band radiative heat dissipation[J]. Light: Science & Applications, 2023, 12(1): 246.
[207] Chu Q Q, Zhang F Y, Zhang Y, et al. Integrated thermal emission microchip based on meta-cavity array[J]. Nanophotonics, 2022, 11(18): 4263-4271.
[208] Chu Q Q, Zhang F Y, Zhang Y, et al. Indirect measurement of infrared absorption spectrum through thermal emission of meta-cavity array[J]. Optics Express, 2023, 31(24): 39832-39840.
[209] Zhang F Y, Chu Q Q, Wang Q, et al. Multiple symmetry protected BIC lines in two dimensional synthetic parameter space [J]. Nanophotonics, 2023, 12(13): 2405-2413.
[210] 李强, 应云斌, 仇旻. 热辐射方向调控研究进展[J]. 光学学报, 2024, 44(19): 1900001.
Li Q, Ying Y B, Qiu W. Research progress of thermal emission direction control[J]. Acta Optica Sinica, 2024, 44(19): 1900001.
[211] 孙雨威, 贺楠, 张智, 等. 吸波超表面及其在中红外波段的应用[J]. 光学学报, 2022, 42(17): 1704001.
Sun Y W, He N, Zhang Z, et al. Absorbing metasurfaces and their applications in the mid-infrared band[J]. Acta Optica Sinica, 2022, 42(17): 1704001.

Thermal Emission Manipulation and Its Infrared Applications Based on Metasurfaces (Invited)

Shang Xiaohe[1], Zhong Fan[2**], Shang Jinguang[1], Zhang Ye[1], Xiao Yanling[1], Zhu Shining[1], Liu Hui[1*]

[1]*School of Physics, National Laboratory of Solid State Microstructures, Collaborative Innovation Center of Advanced Microstructures, Nanjing University, Nanjing* 210093, *Jiangsu, China*;
[2]*School of Physics, Key Laboratory of Quantum Materials and Devices of Ministry of Education, Southeast University, Nanjing* 211189, *Jiangsu, China*

Abstract

Significance As is known, traditional thermal emission is broadband, unpolarized, and incoherent, typically altered by changing temperature to modify spectral line shapes and intensities. Conventional materials face challenges in accurately controlling the radiation characteristics with multiple degrees of freedom, limiting their applications in infrared spectra. In recent years, two-dimensional metasurface structures with sub-wavelength size and ultra-thin thickness have overcome the limitations of traditional research on thermal emission manipulation due to their flexible and controllable optical response. Metasurface structures obtained via various designs have successfully manipulated thermal emission in multiple degrees of freedom, such as wavelength, polarization, direction, time, and coherence. This has promoted the miniaturization and integration of infrared devices.

Progress Both realizing rational wavelength-selective emission and manipulating the emission at other wavelengths as much as possible are essential for practical infrared applications. In 2011, Liu's research group experimentally developed a narrow dual-band mid-infrared thermal emitter [Fig. 1(a)]. In 2013, Argyropoulos' research group discussed the possibility of realizing ultra-broadband omnidirectional absorbers and angularly selective coherent thermal emitters based on properly patterned plasmonic metastructures [Fig. 1(b)]. In 2015, Hossain's group designed and experimentally demonstrated a metamaterial thermal emitter for highly efficient radiative cooling [Fig. 1(c)]. In contrast to unpolarized blackbody thermal emission, metasurface-based thermal emitters with fabricated subwavelength meta-atoms typically emit polarized thermal emission. For linearly polarized thermal emission, Liu's research group experimentally demonstrated a new type of macroscopic perfect and tunable thermal emitters in 2017 [Fig. 2(a)]. Additionally, circularly polarized thermal emission is another hot spot for polarization manipulation of thermal emission. In 2010, Dahan's research group experimentally demonstrated spin-dependent dispersion splitting of the emitted light and analyzed it in terms of a geometric Doppler shift [Fig. 2(b)]. In 2023, Nguyen's research group reported the emission of polarized mid-wave infrared (MWIR) radiation from a 700 nm thick incandescent chiral metasurface [Fig. 2(c)]. In 2023, Wang's research group designed nonvanishing optical helicity by engineering a dispersionless band that emits omnidirectional spinning thermal radiation [Fig. 2(d)]. Further wavelength-selective thermal emission within the demanded emission directions should be restricted to improve the emission efficiency. In 2010, Han's research group theoretically examined thermal emission from metallic films with surfaces that are patterned with a series of circular concentric grooves (a bull's eye pattern) [Fig. 3(a)]. In 2015, Costantini's research group introduced a plasmonic metasurface to control the spectrum and directivity of blackbody radiation [Fig. 3(b)]. In 2021, Overvig's research group introduced a platform for thermal metasurfaces and completed the compactification program of optical systems [Fig. 3(c)]. In 2017, Zhang's research group found that thermal emission of phonon can be controlled by the magnetic resonance mode in a metasurface [Fig. 4(a)]. In 2019, Zhang's research group employed Al/SiN/Al metasurface to manipulate the thermal emission in the infrared range [Fig. 4(b)]. In 2020, Zhong's research group established angle-resolved thermal emission spectroscopy as an alternative platform to characterize the intrinsic eigenmode properties of non-Hermitian systems [Fig. 4(c)]. In 2021, Zhong's research group proposed a scheme to construct and probe the mid-infrared surface wave radiation of the interface state in the waveguide by thermal emission [Fig. 4(d)]. In recent years, dynamic tunable thermal emitters possessing switchable thermal emission properties under high-speed modulation have caught extensive attention to develop adaptive thermal management devices. In 2019, Kang's research group demonstrated the electrical modulation of a narrowband MWIR thermal emission at high temperatures of up to 500 ℃ by adopting GaN/AlGaN multiple quantum well photonic crystals [Fig. 5(a)]. In 2017, Liu's research group proposed and demonstrated the idea of a metamaterial microelectromechanical system capable of tailoring the energy emitted from a surface [Fig. 5(b)]. In 2017, Coppens' research group achieved simultaneous spatio-temporal emission manipulation [Fig. 5(c)]. In 2021, Xu's research group experimentally demonstrated a nonvolatile optically reconfigurable mid-infrared coding radiative metasurface [Fig. 5(d)]. The nonreciprocal system is fundamentally vital for solar energy harvesting systems to reach their efficiency limit and is appealing to thermal management devices, which are usually designed by following Kirchhoff's law. In 2014, Zhu's research group validated general principles by direct numerical calculations based on fluctuational electrodynamics and thermal emitters constructed from magneto-optical photonic crystals [Fig. 6(a)]. In 2020, Zhao's research group indicated that the axion electrodynamics in magnetic Weyl semimetals can be adopted to construct strongly nonreciprocal thermal emitters that nearly completely violate Kirchhoff's law overbroad angular and frequency ranges without requiring any external magnetic field [Fig. 6(b)]. In 2022, Ghanekar's research group exploited spatio-temporal refractive index modulation of a grating to drive photonic transitions between guided resonance modes [Fig. 6(c)]. The above-mentioned studies have been conducted to study far-field thermal emission, which is bounded by the Planck thermal-emission limit. However, subwavelength thermal emitters appear to exceed the limit. In 2015, Liu's research group investigated the near-field radiative heat transfer of 1D and 2D metasurfaces [Fig. 7(a)]. In 2017, Fernández-Hurtado's research group proposed a novel mechanism to further enhance near-field radiative heat transfer (NFRHT) with the utilization of Si metasurfaces [Fig. 7(b)]. In 2017, Shi's research group proposed multilayer graphene-hBN heterostructures to further enhance the near-field thermal radiation [Fig. 7(c)]. In 2018, Ilic's research group theoretically demonstrated a near-field radiative thermal switch based on thermally excited surface plasmons in graphene resonators [Fig. 7(d)]. Numerous research on manipulating thermal emission has brought new perspectives for various infrared applications, including radiative cooling, thermophotovoltaic devices, thermal camouflage, thermal imaging, and biochemical sensing. In 2013, Rephaeli's research group presented a metal-dielectric photonic structure capable of radiative cooling in daytime outdoor conditions [Fig. 8(a)]. In 2017, Zhai's research group demonstrated efficient day and nighttime radiative cooling with a randomized and glass-polymer hybrid metamaterial [Fig. 8(b)]. In 2021, Zeng's research group demonstrated a hierarchically designed polymer nanofiber-based film, which enables selective mid-infrared emission, effective sunlight reflection, and excellent all-day radiative cooling performance [Fig. 8(c)]. In 2018,

Chang's research group demonstrated tungsten-based refractory metasurfaces with desired spectral selectivity for solar thermophotovoltaics (STPVs) applications [Fig. 8(d)]. In 2018, Salihoglu's research group reported a new class of active thermal surfaces enabling efficient real-time electrical control of thermal emission over the full infrared spectrum without changing the surface temperature [Fig. 8(e)]. Thermal emission manipulation in multiple degrees of freedom is mostly performed on a single metasurface, therefore resulting in limited capabilities of manipulating thermal emission. Further extending the manipulation degrees of freedom is essential for practical infrared applications. A pixelated metasurface array is a promising solution to this problem. In 2022, Chu's research group proposed a micro-meta-cavity array by combining nanohole metasurfaces and Fabry-Pérot cavity [Fig. 9(a)]. Polarization, wavelength, and spatial multiplexing thermal emission with high spatial resolution have also been experimentally demonstrated by utilizing nanohole patterns. In 2023, Chu's research group experimentally demonstrated an integrated technology that allows for indirect absorption spectrum measurement via thermal emission of a meta-cavity array. This indirect measurement method opens a new avenue for compact infrared spectroscopy analysis.

Conclusions and Prospects Wavelength-selective thermal emission is the key to improving the efficiency of various thermal management applications. Metasurface-based thermal emitters have successfully achieved the emission spectrum required by plenty of infrared devices. Meanwhile, we discuss the flexible manipulation of the radiation angle, polarization, and coherence properties of thermal emission, with a focus on nonreciprocal thermal emission and near-field thermal emission research. An integrated metasurface array on a single chip can be utilized promisingly to obtain more tunable degrees of freedom. Given that integration and miniaturization are the development goals for future flat and compact infrared applications, there are still several challenges for on-chip thermal emission manipulation. In recent years, various interesting physics mechanisms have been explored and applied to optical research.

Key words metasurface; metasurface array; thermal emission manipulation; infrared application